

©2019

Robert J. Cannon

ALL RIGHTS RESERVED

**QUANTITATION OF KEY ODORANTS IN
ARGININE/CYSTEINE-GLUCOSE MAILLARD REACTIONS**

by

ROBERT J. CANNON

A thesis submitted to the

School of Graduate Studies

Rutgers, The State University of New Jersey

In partial fulfillment of the requirements

For the degree of

Master of Science

Graduate Program in Food Science

Written under the direction of

Dr. Chi-Tang Ho

And approved by

New Brunswick, New Jersey

MAY 2019

ABSTRACT OF THE THESIS

Quantitation of Key Odorants in Arginine/Cysteine-Glucose Maillard Reactions

by ROBERT J. CANNON

Thesis Director:

Dr. Chi-Tang Ho

Unlike many other named reactions in organic chemistry, the Maillard reaction is not a clearly defined single pathway. Instead, it is one of the most complex processes in food chemistry. Maillard reactions studied in the literature over the last fifty years have focused either on simple model systems or complex culinary processes. The next step in our understanding of Maillard reactions is to bridge the gap between these simple and complex systems. By adding more than one amino acid to a model system, we aim to better understand the different mechanisms for which certain aroma compounds are formed.

In this study, L-arginine and L-cysteine were selected as the two amino acids in the thermal reaction with glucose. Found most abundantly in turkey and chicken, arginine is a basic, polar amino acid that has not been well studied in terms of its generation of volatile compounds from the Maillard reaction. In contrast, L-cysteine, an amino acid found in meat and poultry, has been studied in detail. Using different reaction conditions, the key odorants from several arginine-cysteine/glucose model studies were identified and quantified by gas chromatography-mass spectrometry (GC-MS) and gas chromatography-olfactometry (GC-O).

Attention was given to the extraction procedure used for the isolation of the aroma compounds. The methodology of Likens-Nickerson extraction, better known as steam distillation extraction (SDE), has often been used in the literature to isolate the aroma compounds from Maillard reactions. A comparison of several data sets will show that solvent assisted flavor evaporation (SAFE) is a more preferred method for the isolation and recovery of a wide range of key odorants. This is evident in the quantitation of hydrophilic, mercapto acids, including 2-mercaptopropionic acid and 3-mercaptopropionic acid. The physico-chemical properties ($\log_{10}P_{ow}$) and the mechanisms of formation will be discussed for both compounds.

Finally, the mechanisms of formation for additional key odorants identified by GC-MS and GC-O will be proposed. A strategy to prove these mechanisms and ideas for supplementary reactions will be briefly discussed.

Acknowledgement

As I reflect on my last few years at Rutgers, I am reminded of how fortunate I am to have the family, friends, and professors that have supported this journey. I certainly had my doubts embarking on this challenge. At the time, it had been ten years since I completed my last undergraduate chemistry class. I vividly remember the moment when I first entered Food Chemistry Fundamentals in 2015 where I felt both terrified and excited at the same time. There were many times the last few years that I questioned if a subject was just too far removed from my memory or if I could continue with work and family obligations. Each time there were family, friends, and professors that helped to rally me to the finish line. I am forever grateful to them.

I am especially thankful to Dr. Chi-Tang Ho who has been an incredible advisor and friend. His kindness and compassion for me and all his students is unparalleled. I always looked forward for each time we met to go over research, discuss classes, or just talk about chemistry and his experiences. To be able to work with Dr. Ho, a legend in food chemistry, has been one of the biggest highlights of my career.

Finally, my biggest thank you goes to my wife and three kids. All the late nights in class and the long weekends cooped up in a library meant time away from them. They sacrificed so much and were always supportive and loving. Thank you for allowing me to do this.

Table of Contents

Abstract of the Thesis	ii
Acknowledgment.....	v
Table of Contents	vi
List of Figures.....	viii
List of Tables.....	xi
Introduction.....	1
1.1 Maillard Reaction.....	1
1.1.1 Background.....	1
1.1.2 Arginine in the Maillard Reaction	4
1.1.3 Cysteine in the Maillard Reaction.....	10
1.2 Isolation of Volatile Compounds.....	15
1.2.1 Background.....	15
1.2.2 Steam Distillation.....	15
1.2.3 Solvent Assisted Flavor Evaporation.....	17
1.2.4 Static and Dynamic Headspace	19
Hypothesis and Objectives	21
2.1 Hypothesis	21
2.2 Research Objectives	23
Experimental	24
3.1 Materials	24
3.2 Instruments	24
3.3 Methods	25

3.3.1 Preparation of Maillard Reactions	25
3.3.2 Liquid-Liquid Extraction of Maillard Reaction	26
3.3.3 Solvent Assisted Flavor Evaporation of Maillard Extracts	27
3.3.4 Steam Distillation Extraction of Maillard Reaction	28
3.3.5 GC Analysis of Maillard Extracts	28
3.3.6 GC-MS Analysis of Maillard Extracts	29
3.3.7 GC-O Analysis of Maillard Extracts	30
3.3.8 NMR Analysis	31
3.3.9 Measurement of Partition Coefficients by HPLC	31
Results	33
4.1 Maillard Reaction of Arginine-Glucose	33
4.1.1 Identification of Hydroxyethyl Pyrazines	39
4.1.2 Proposed Mechanism of Formation of Hydroxyethyl Pyrazines	43
4.2 Maillard Reaction of Cysteine-Glucose	47
4.2.1 Comparison of SAFE and SDE in Cysteine-Glucose Reaction.....	54
4.2.2 Formation of Mercapto Acids	60
4.2.3 Physico-Chemical Properties of Mercapto Acids	62
4.3 Maillard Reaction of Arginine/Cysteine-Glucose.....	64
Conclusions.....	70
5.1 Future Work	70
References	73
Appendix.....	85

List of Figures

Figure 1.1 The subdivisions of the Maillard Reaction (adapted from Hodge, 1953).

Figure 1.2 The two major pathways from the Amadori intermediate depending on pH (adapted from Nursten, 2005).

Figure 1.3 The chemical structure of L-arginine.

Figure 1.4 The general pathway to produce Strecker aldehydes in the Maillard reaction.

Figure 1.5 Structures of (A) glyoxal and (B) methylglyoxal.

Figure 1.6 (A) The reaction of 1,2-cyclohexanedione and arginine (Pathy & Smith, 1975); (B) the product of reacting glyoxal and arginine (Schwarzenbolz, Henle, Haefner & Klostermeyer, 1997).

Figure 1.7 Arginine reacted with either methylglyoxal or 3-deoxyglucosenone (3-DG) to form two imidazolone derivatives (adapted from Zhu & Yaylayan, 2017).

Figure 1.8 The chemical structure of L-cysteine.

Figure 1.9 Six of the most odor active compounds in the reaction of cysteine and ribose: (A) furfuryl mercaptan; (B) 3-mercaptopentan-2-one; (C) 2-methylfuran-3-thiol; (D) 5-acetyl-2,3-dihydro-1,4-thiazine; (E) 3-mercaptobutan-2-one; (F) bis-(2-methyl-3-furyl)-disulfide (adapted from Hofmann & Schieberle, 1995).

Figure 1.10 The Strecker degradation of L-cysteine to form mercaptoacetaldehyde and cysteamine.

Figure 1.11 An image of a Likens-Nickerson distillation apparatus.

Figure 1.12 An image of a SAFE apparatus (image adapted from Engel, Bahr & Schieberle, 1999).

Figure 1.13 An image of solid-phase microextraction (SPME; image adapted from Vas & Vekey, 2004).

Figure 2.1 Predicted formation of the Strecker aldehyde derived from the reaction of methyl glyoxal and arginine.

Figure 3.1 An image of a SAFE setup used to isolate the volatile fraction of the diethyl ether extract.

Figure 4.1 Four reactions of Arg-Glu. From left to right: Arg-Glu at 100 °C at pH 7.4; Arg-Glu at 130 °C at pH 7.4; Arg-Glu at 160 °C at pH 7.4; Arg-Glu at 160 °C at pH 10.4.

Figure 4.2 The spectra and predicted fragmentation pattern of (A) 2-(pyrazin-2-yl)ethan-1-ol and (B) 2-(5-methylpyrazin-2-yl)ethan-1-ol based on the elemental composition of the molecular ion and associated fragments from exact mass measurements.

Figure 4.3 Proposed formation of (A) 2-(pyrazin-2-yl)ethan-1-ol; (B) 2-(5-methylpyrazin-2-yl)ethan-1-ol; and (C) 2-(6-methylpyrazin-2-yl)ethan-1-ol.

Figure 4.4 Proposed formation of (A) 2-vinylpyrazine (CAS 4177-16-6); (B) 2-methyl-6-vinylpyrazine (CAS 13925-09-6); and (C) 2-methyl-5-vinylpyrazine (CAS 13925-08-1) by water elimination of the respective hydroxyethyl pyrazine.

Figure 4.5 Two reactions of Cys-Glu. From left to right: Cys-Glu at 130 °C at pH 7.4; Cys-Glu at 160 °C at pH 7.4.

Figure 4.6 The structures of (A) 2,5-dimethyl-4-hydroxy-3(2H)-thiophenone (DMHT) and (B) 2,5-dimethyl-2,4-dihydroxy-3(2H)-thiophenone (DMDHT).

Figure 4.7 The structures and odor descriptors of 2MPA and 3MPA from the Cys-Glu reaction.

Figure 4.8 The formation of 3MPA by transamination of 2-oxo-3-mercaptopropionic acid and reduction of alpha-keto acid (adapted from Tressl, Kersten, Nittka & Rewicki, 1994).

Figure 4.9 The formation of 2MPA by beta-elimination of hydrogen sulfide (adapted from Tressl, Kersten, Nittka & Rewicki, 1994).

Figure 4.10 Three reactions of Arg/Cys-Glu. From left to right: Arg/Cys-Glu at 100 °C at pH 7.4; Arg/Cys-Glu at 130 °C at pH 7.4; Arg/Cys-Glu at 160 °C at pH 7.4.

Figure 5.1 Examples of epigallocatechin-3-gallate (EGCG) reacting with one or two equivalents of methylglyoxal (MGO) in both the 6- and 8-position of the polyphenol (adapted from Wang & Ho, 2012).

List of Tables

Table 4.1 The analytical data from the Arg-Glu reactions.

Table 4.2 The analytical data from the Cys-Glu reactions at two different reaction temperatures.

Table 4.3 The analytical data from SDE and SAFE extracts of the Cys-Glu reactions.

Table 4.4 A comparison of high impact, low concentration sulfur compounds in both the SDE and SAFE extracts.

Table 4.5 A comparison of high impact, high concentration sulfur compounds in both the SDE and SAFE extracts.

Table 4.6 The measured $\log_{10}P_{ow}$ values for duplicate measurements of 2MPA and 3MPA.

Table 4.7 The analytical data from the Arg/Cys-Glu reactions.

Introduction

1.1 Maillard Reaction

1.1.1 Background

Non-enzymatic browning reactions have been studied and reviewed since the early twentieth century (Hodge, 1953). The Maillard reaction is one of three types of non-enzymatic browning reactions that can occur in foods (caramelization and ascorbic acid oxidation being the other two) and has garnered immense research due to the incredibly complex mechanisms and products formed that generate flavor, color, and physiological consequences. Compared to other named reactions in organic chemistry, the Maillard reaction is not a clearly defined single reaction. Instead, it comprises several reactions (rearrangement, fragmentation, degradation, dehydration) as shown in Figure 1.1.

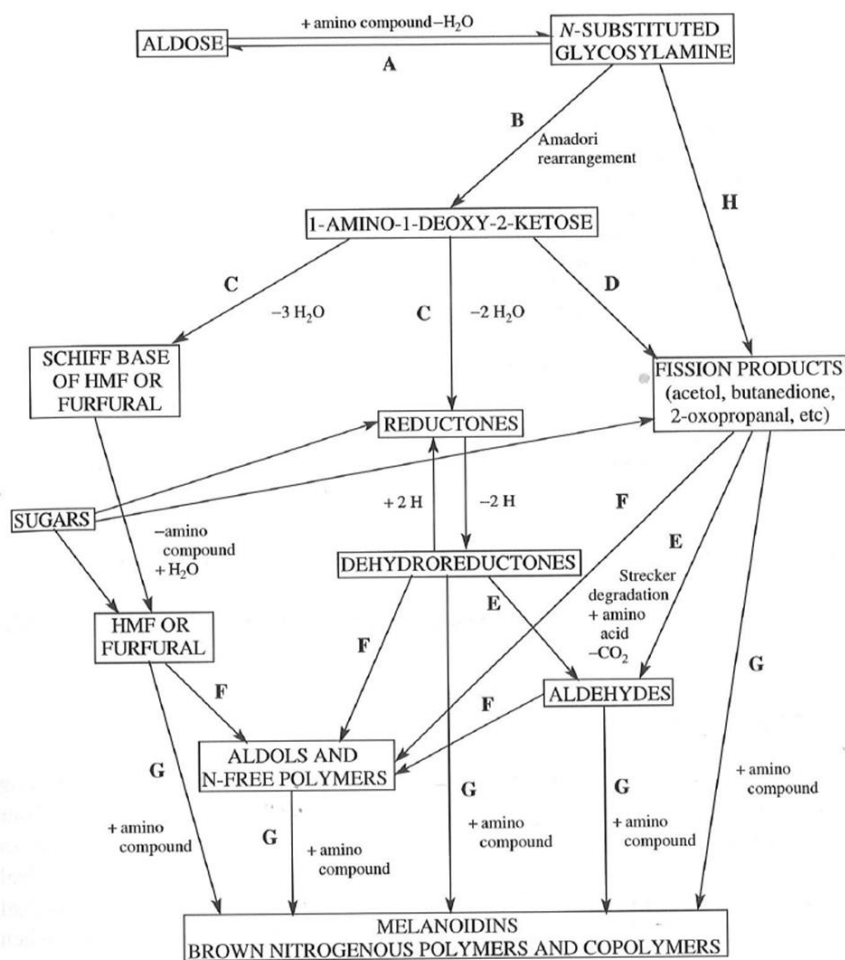


Figure 1.1 The subdivisions of the Maillard Reaction (adapted from Hodge, 1953).

The initial stage of the reaction is driven by the condensation of a reducing sugar and an amino compound. The amino compound could be free amino acids, peptides, lysine residues from a protein, phosphatidyl ethanolamine or free ammonia. This condensation product can then generate a cascade of reactive intermediates (eg Amadori rearrangements) which ultimately produce aroma, flavor, and color compounds in foods. The formation of final products from the Amadori intermediates depend mainly on the pH of the system. At low pH, the route of 1,2-enolisation via 3-

deoxy-1,2-carbonyls is favored. At high pH, 2,3-enolisation via 1-deoxy-2,3-carbonyls is favored as shown in Figure 1.2 (Nursten, 2005).

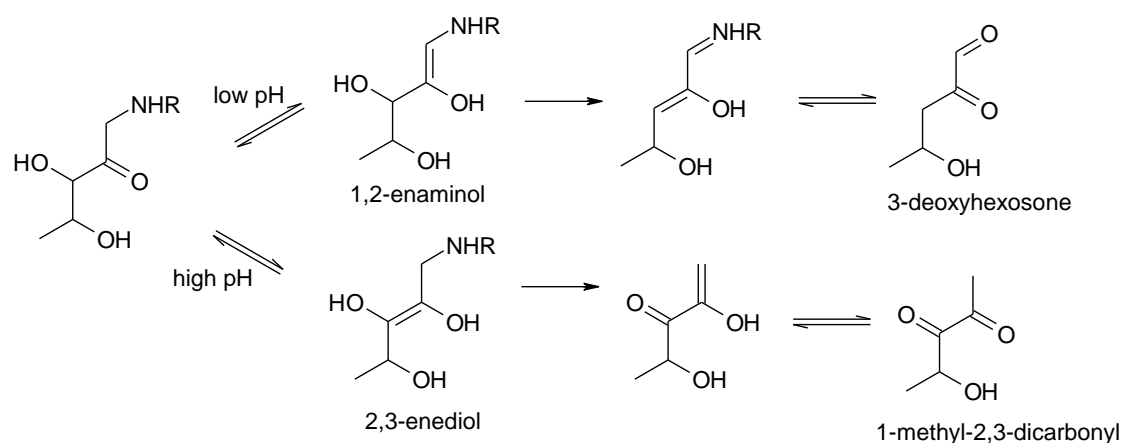


Figure 1.2 The two major pathways from the Amadori intermediate depending on pH (adapted from Nursten, 2005).

For simple Maillard model systems, the mechanisms for which volatiles are generated depend principally on the pH, temperature, amount of oxygen, and the concentration of amino acid and reducing sugar. One could imagine how complicated the reactions and mechanisms for which volatiles are generated in more complex Maillard systems, where there could be multiple amino acids and reducing sugars, as well as proteins, lipids, polyphenols, and other chemical constituents in natural foodstuffs. The more we continue to learn and document the analytical and sensory data from complex Maillard reactions, the better chance of guiding product development to deliver high impact ingredients in high purity from these processed reactions (Lund & Ray, 2017; Mottram & Elmore, 2010).

1.1.2 Arginine in the Maillard Reaction

L-Arginine, a basic amino acid with a positively charged guanidino group, found in many animal sources (meats, fish, eggs) and plant sources (nuts, grains, seeds). This amino acid contains both an α - and ϵ -amino groups and has an isoelectric point at pH 10.8 (see Figure 1.3).

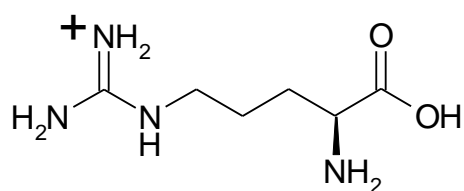


Figure 1.3 The chemical structure of L-arginine.

In the literature, only a few references discuss the chemistry and kinetics of arginine in the Maillard reaction. In fact, no reference has yet to identify the Strecker aldehyde of arginine. Strecker aldehydes are an important class of flavor chemicals that provide common aromas in foods. For example, methional (Strecker aldehyde from L-methionine) is a key aroma compound in potatoes, while isovaleraldehyde (Strecker aldehyde from L-leucine) and 2-methylbutanal (Strecker aldehyde from L-isoleucine) are important odorants in chocolate. Strecker aldehydes are formed from the reaction of free amino acids and α -dicarbonyl compounds, which are typically Maillard reaction intermediates from thermal processing. The general pathway is shown in Figure 1.4.

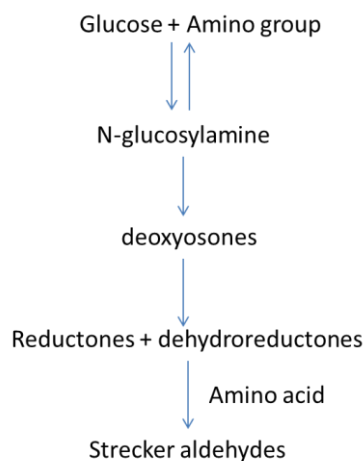


Figure 1.4 The general pathway to produce Strecker aldehydes in the Maillard reaction.

In this reaction, an α -carbonyl compound reacts with the amino group of an amino acid to form a Schiff base, which will undergo further degradation by decarboxylation and deamination of the amino acid to form Strecker aldehydes.

Arginine has been often studied for its ability to be reversibly modified with α,α' -dicarbonyl compounds including 1,2-cyclohexanedione (Toi, Bynum, Norris & Itano, 1967; Patthy & Smith, 1975), phenylglyoxal (Takahashi, 1968), glyoxal (Schwarzenbolz, Henle, Haefner & Klostermeyer, 1997; Glomb & Lang, 2001), methylglyoxal (Klopfer, Spanneberg & Glomb, 2011), and 3-deoxyglucosone (Hayase, Konishi & Kato, 1995). Glyoxal and methylglyoxal (see Figure 1.5), both degradation products of reducing sugars like glucose, are highly reactive carbonyl compounds that are responsible for color and flavor generation in the Maillard reaction (Wang & Ho, 2012).

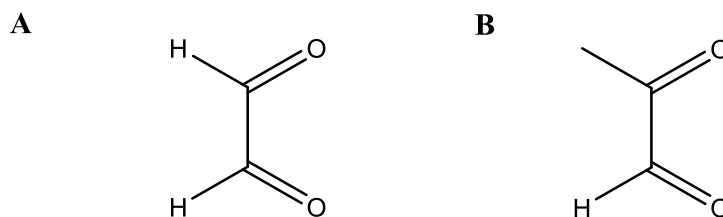


Figure 1.5 Structures of (A) glyoxal and (B) methylglyoxal.

The condensation products of these α,α' -dicarbonyl compounds with the guanidine group have been identified and often characterized for their ability to limit the hydrolysis by trypsin, an enzyme that acts in the hydrolysis of peptide bonds. Two examples of these reactions are shown in Figure 1.6.

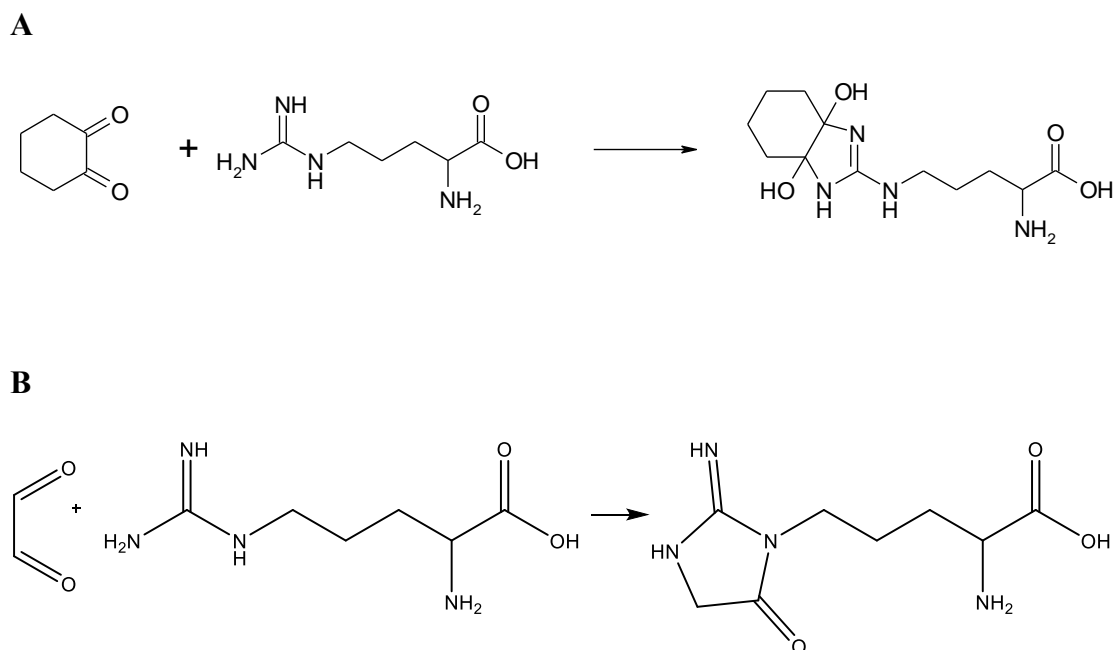


Figure 1.6 (A) The reaction of 1,2-cyclohexanedione and arginine (Patthy & Smith, 1975); (B) the product of reacting glyoxal and arginine (Schwarzenbolz, Henle, Haefner & Klostermeyer, 1997).

More recently, research by Zhu & Yaylayan investigated the reactivity of guanidine and arginine with glucose (Zhu & Yaylayan, 2017). Results showed that free guanidine will condense with one, two, or three glucose molecules. However, the authors results showed that the guanidine group of arginine could not be released during the Maillard reaction, so these condensation Amadori rearrangement products would not form. For the reaction of arginine and glucose, the authors identified Amadori products at the α - and ϵ -amino groups. At the ϵ -amino group, arginine reacted with methylglyoxal and 3-deoxyglucosone (Maillard intermediates) to form imidazolone derivatives (Figure 1.7).

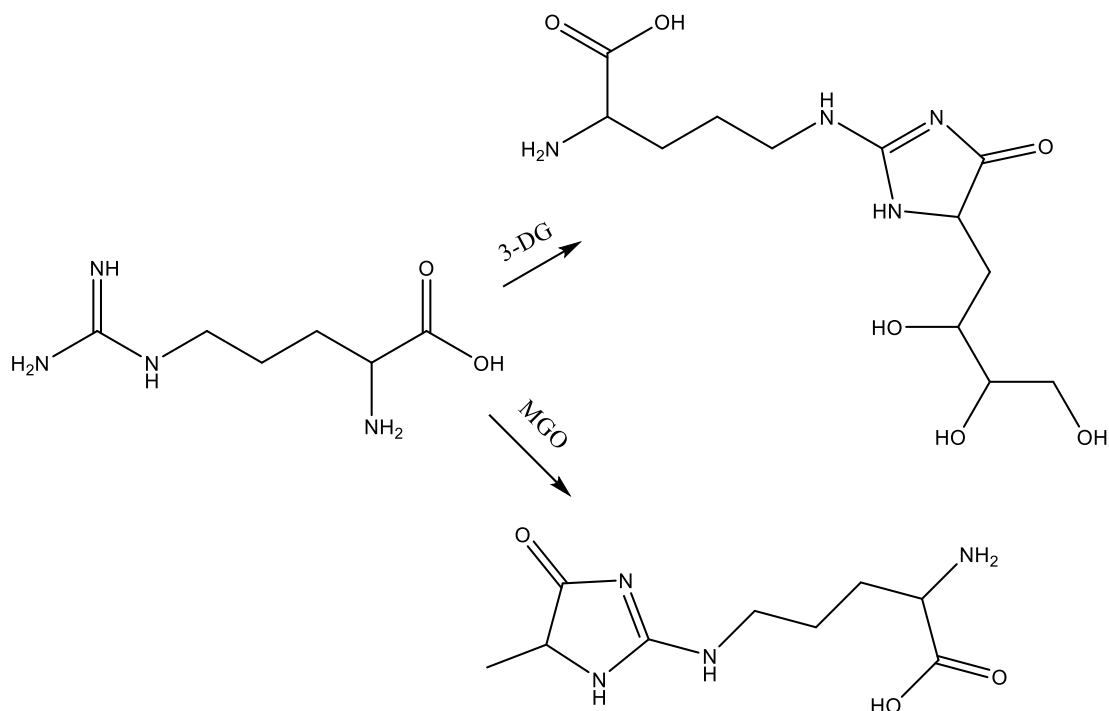


Figure 1.7 Arginine reacted with either methylglyoxal or 3-deoxyglucosone (3-DG) to form two imidazolone derivatives (adapted from Zhu & Yaylayan, 2017).

Additional studies in the literature focused on the reactivity and kinetics of L-arginine compared to other amino acids in the Maillard reaction. In the reaction of either diacetyl, glucose, fructose, or methylglyoxal, Piloty & Baltes found L-arginine to be the most reactive out of the thirteen amino acids studied (Piloty & Baltes, 1979). Takahashi studied rate of reactions with amino acids and phenylglyoxal, glyoxal, and methyl glyoxal (Takahashi, 1977). L-arginine was identified as the most reactive amino acid, and the rate of the reaction increased with increasing pH. The author's results showed that the ϵ -amino group of L-arginine is more reactive compared to the α -amino group. In addition, results showed that this reaction was selective for just L-arginine, while lysine which also contains an ϵ -amino group, did not react with phenylglyoxal.

Additional work done later by Hwang et al. seemed to contradict this result (Hwang, Hartman, Rosen, Lech & Ho, 1994). Using isotope labeled lysine, the authors showed that in fact both amino groups were involved in dry and aqueous Maillard reactions to form pyrazine compounds, and the α -amino group reacted more readily compared to the ϵ -amino group.

Several research efforts studied the chemistry and kinetics of pyrazine formation in different amino acid model systems. In 1989, Huang et al. measured the volatile constituents from the aqueous reaction of four amino acids (glycine, lysine, histidine, arginine) with glucose at equimolar concentrations at pH 10 (Huang, Bruechert & Ho, 1989). The authors most likely chose this pH because the initial condensation of amino acids and carbonyl groups is favored under basic conditions, thus allowing for the rearrangement and fragmentation of glucose to generate a higher yield of pyrazines. The results from this study offered that arginine produced the highest concentration of alkylpyrazines (2-methylpyrazine being the most abundant). Later, Hwang et al. studied the generation of pyrazines from the interaction of two different amino acids with glucose in a dry system at pH 7 (Hwang, Hartman & Ho, 1995). Reaction mixtures containing the combination of equimolar concentration of glycine and arginine produced the lowest yield of pyrazines compared to the other seven tested amino acids. The data clearly showed that arginine inhibited the ability of glycine to produce pyrazines. Interestingly, the reaction of glycine and lysine produced the highest yield of pyrazines, suggesting a synergistic response. The differences in the yield of pyrazines from Huang et al. in 1989 and Hwang et al. in 1995 are expected. In the latter study, the authors conducted the reaction at pH 7, where the basic ϵ -amino group is ionized and unreactive, thereby contributing very little to catalyze sugar fragmentation

and Strecker degradation. In contrast, lysine always has a fraction of nonionized amino groups (Creighton, 1984) which will readily react under Maillard conditions and generate higher concentrations of pyrazines. The relative reactivities of these amino acids were further documented in a follow up study by Hwang et al. when the authors measured higher concentrations of pyridines, pyrroles, and oxazoles in lysine-glycine reactions compared to arginine-glycine reactions (Hwang, Hartman & Ho, 1995b).

1.1.3 Cysteine in the Maillard Reaction

In comparison to L-arginine, L-cysteine has been well-studied in the Maillard reaction. L-cysteine is a sulfur-containing amino acid (Figure 1.8) with an isoelectric point at pH 5.1. Essential to meat flavors, L-cysteine can generate a significant amount of both hydrogen sulfide and ammonia through several pathways (Kobayasi & Fujimaki, 1965; Sohn & Ho, 1995). Hydrogen sulfide and ammonia can then react with many secondary volatiles including carbonyl compounds to produce high impact odorants including thiols, pyrazines, thiazolines, and thiazoles.

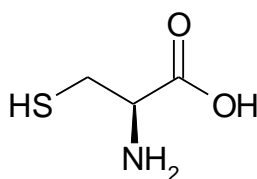


Figure 1.8 The chemical structure of L-cysteine.

Arguably the most important method to identify odor active compounds from any

reaction or natural product extract is GC-O. Even with the recent advances to the sensitivity and resolving power of GC-MS instruments, the human nose is still more sensitive and irreplaceable to the characterization of these reactions. Important techniques have been developed that utilize GC-O to help identify the key odorants, including Charm analysis (Acree, Barnard & Cunningham, 1984) and Aroma Extract Dilution Analysis (AEDA) (Schieberle & Grosch, 1987). Using AEDA, an extract is injected onto a GC-O and stepwise diluted by a factor of two or three until odorants are no longer detected by the human olfactory system. Each odorant is then assigned a flavor dilution (FD) factor based on these dilutions. This is a qualitative method of numerically representing the strength of the odor. For example, a calculation can begin with the formula, 3^n , where 3 is the dilution factor (3-fold) and n is the last dilution the odor was detected. A compound detected by odor up to the fourth dilution would have FD of 3^4 or 81. AEDA assists in the initial determination of which compounds may have the highest contribution or potency to the aroma profile of the food product. The FD factors of each compound, along with its respective concentrations, provide valuable insights into key odorants of that extract.

Stable isotope dilution analysis (SIDA) was first developed by Sweeley et al. (Sweeley, Elliott, Fries & Ryhage, 1966) and later for the flavor and fragrance industry by Schieberle & Grosch (Schieberle & Grosch, 1987b). There can be significant losses of certain compounds during the extraction and isolation of either volatile or non-volatile compounds from a food matrix. To correct for these losses, SIDA is implemented to measure extraction recoveries and to accurately quantify the compounds of interest. For example, a preliminary extraction using an internal standard can be done on a product to identify the key odorants by GC-O and AEDA. The internal standard will

provide semi-quantitative data for the concentration of the key odorants. Next, a second extraction of the same sample is made with the deuterated or carbon-13 labeled odorants, many of which are now commercially available, that have a high flavor dilution factor by AEDA. These deuterated odorants are spiked into the food product at the approximate level each were qualitatively measured in the preliminary extraction. The same extraction is applied to accurately quantify those specific compounds using the deuterated derivative standards. These standards should experience the same losses during extraction and purification and help to provide accurate quantities of the key odorants in the food.

The volatile compounds generated from the reaction of L-cysteine with different reducing sugars have been detailed in numerous papers over the years, including cysteine-xylose (Tressl, Helak, Martin & Kersten, 1989; de Roos, Wolswinkel & Sipma, 2005), cysteine-glucose (Tressl, Helak, Martin & Kersten, 1989; Kato, Kurata & Fujimaki, 1973), cysteine-arabinose (Tressl, Kersten, Nittka & Rewicki, 1994), cysteine-rhamnose (Hofmann & Schieberle, 1997; Hofmann & Schieberle 1998), cysteine-ribose (Mulders, 1973; Zhang & Ho, 1991; Mottram & Nobrega, 2002; Cerny & Davidek, 2003). In the thermal reaction (145 °C) of cysteine and ribose, 29 odor-active volatiles were identified by GC-O and AEDA through the work of Hofmann & Schieberle (shown in Figure 1.9) (Hofmann & Schieberle, 1995).

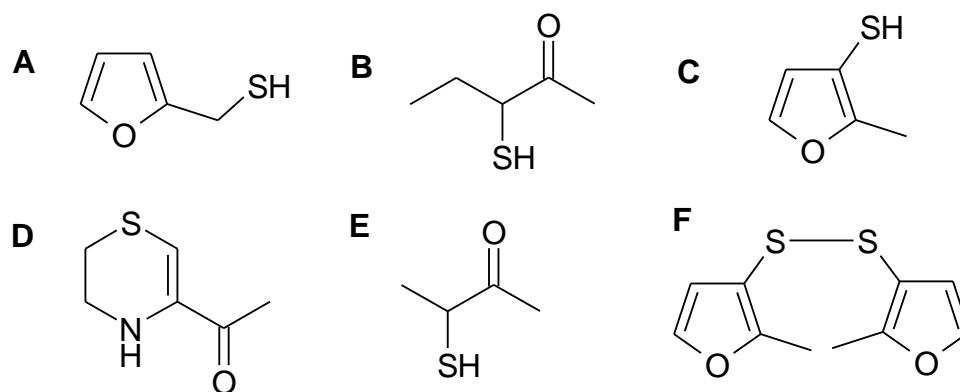


Figure 1.9 Six of the most odor active compounds in the reaction of cysteine and ribose: (A) furfuryl mercaptan; (B) 3-mercaptopentan-2-one; (C) 2-methylfuran-3-thiol; (D) 5-acetyl-2,3-dihydro-1,4-thiazine; (E) 3-mercaptobutan-2-one; (F) bis-(2-methyl-3-furyl)-disulfide (adapted from Hofmann & Schieberle, 1995)

The same authors continued to study these reactions with different carbohydrates in both aqueous and dry heated systems (Hofmann & Schieberle, 1997; Hofmann & Schieberle, 1998). The intensity of the odorants using AEDA varied significantly. For example, pyrazines were not detected by GC-O in the aqueous systems for all three carbohydrate systems. However, in the dry heated treatments, pyrazines contributed significantly to the odor of the reaction. In addition, the dry heated conditions of cysteine-ribose produced a FD factor of furfuryl mercaptan four times that of the aqueous cysteine-ribose reaction (FD – 16384 for the dry heated; FD – 4096 for the aqueous heated). Additional studies have shown that temperature, pH, electrolyte concentration, and water activity all affect flavor formation. Shibamoto & Yeo, for example, studied the cysteine-glucose reaction in microwave and conventional ovens (Shibamoto & Yeo, 1993). The results showed a significantly lower concentration of pyrazines and sugar degradation products in the microwave processing

Strecker degradation is an important reaction that generates many of the key compounds from amino acids. In this reaction, an amino acid undergoes oxidative deamination and decarboxylation in the presence of a dicarbonyl compound. An example of the formation of the Strecker aldehyde of L-cysteine is mercaptoacetaldehyde, which is shown in Figure 1.10.

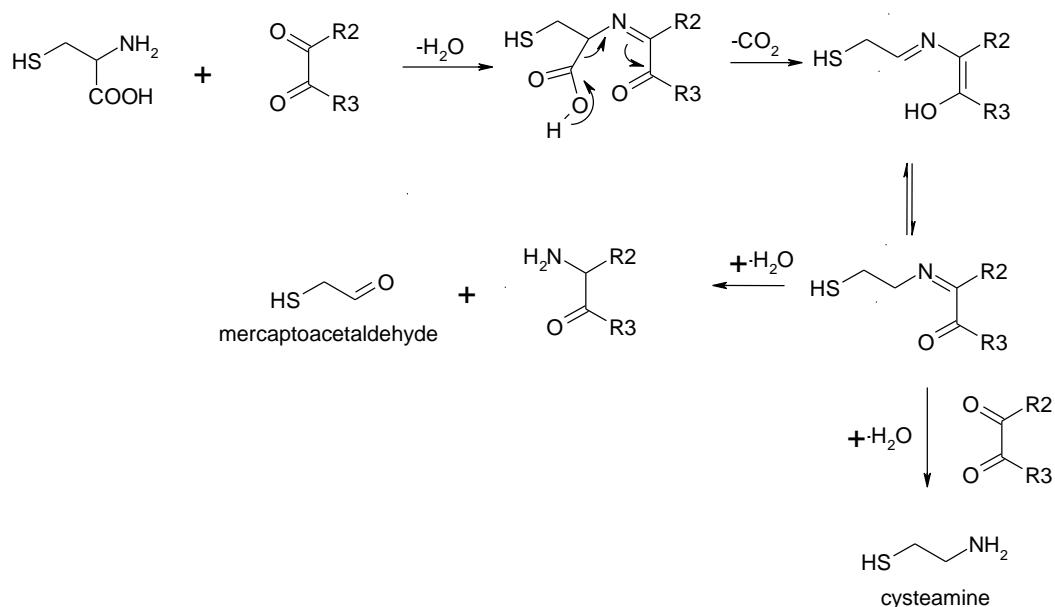


Figure 1.10 The Strecker degradation of L-cysteine to form mercaptoacetaldehyde and cysteamine.

Strecker degradation products can also be highly reactive, allowing for a cascade of additional reactions that could form a range of sulfur and nitrogen compounds that are critical to meat aroma. Mercaptoacetaldehyde, for example, can react with unsaturated aldehydes to form substituted thiophenes (Mulders, 1973). The labile

mercaptoacetaldehyde could also further break down to acetaldehyde and hydrogen sulfide, both of which are important reactants for meat flavors.

1.2 Isolation of Volatile Compounds

1.2.1 Background

There are a multitude of extraction and isolation methods for the identification and quantitation of volatile compounds from Maillard reactions. When it comes to the analysis of these complex types of reactions, it is difficult to measure the efficiency or effectiveness of a specific extraction process especially in terms of the recovery of individual compounds. In terms of a flavor formulation with compounds at known concentrations in a particular matrix, it becomes significantly easier to measure how well a specific extraction process recovers each compound. But for Maillard reactions and natural products, the compounds targeted for extraction in a matrix are often unknown and vary in terms of molecular weight, solubility, and polarity. One qualitative approach is to produce an extract through liquid-liquid extraction (LLE) and compare the smell of the extract with a paper blotter. However, this is more difficult when the isolation of the volatiles is something other than LLE, for example solid phase micro-extraction (SPME) or stir bar sorptive extraction (Sandra, Baltussen, David & Cramers, 1999). A quick review of the major extraction and adsorbent techniques used to study Maillard reactions will be discussed in the next few sections.

1.2.2 Steam Distillation

Likens-Nickerson distillation, more commonly known as steam distillation extraction (SDE), is often utilized in the isolation of the volatile compounds from Maillard reactions (Samsudin, Rongtao & Said, 1996; Zhang, Dorjpalam & Ho, 1992). Developed by Likens & Nickerson in the mid-1960s, the design of the unit allows for a continuous extraction of the condensed vapors of the volatile compounds in the aqueous sample solution with the condensed vapors of a solvent (Likens & Nickerson, 1964). An image of the apparatus is shown in Figure 1.11. The left arm, attached with a round bottom flask, is heated to the boiling temperature of the organic solvent. In the right arm, an aqueous product is heated to its boiling temperature. In the center, a cold finger condenses both the vapors of the solvent and the aqueous product, thereby allowing the volatile compounds to be released from the water phase and extracted by the solvent. There are advantages and disadvantages to this method. SDE recovers a wide range of boiling points and yields a clean extract free from non-volatiles. There are some drawbacks however as the heat processing to generate vapors from the aqueous solution risks thermal decomposition and artifact formation. More recently, reduced pressure SDE has been used as an alternative to atmospheric SDE to limit the high temperature processing (Chaintreau, 2001). Another disadvantage of using SDE is that hydrophilic compounds are less likely to be liberated in the vapor phase, which would ultimately lower the extraction efficiency for those types of compounds.



Figure 1.11 An image of a Likens-Nickerson distillation apparatus.

1.2.3 Solvent Assisted Flavor Evaporation

The current industry standard to isolate and enrich the volatile constituents from a product with nonvolatile components (lipids, colors, etc) is solvent assisted flavor evaporation (SAFE) (Engel, Bahr & Schieberle, 1999). An image of the evaporation apparatus is shown in Figure 1.12. First, either an extract or aqueous solution is introduced dropwise from part A of the apparatus to the round bottom flask on the left (part B). Under high vacuum ($\sim 5 \times 10^{-5}$ Torr) using a diffusion pump, the extract is gently heated to 35-40 °C (depending on the solvent) in an external water bath. The volatile compounds are distilled through the apparatus, which is similarly thermostated to the temperature of the water bath. The distillate is transferred to the round bottom flask on the right part of the apparatus (part C), which is submerged in liquid nitrogen. Any volatiles not first collected in the round bottom flask can be trapped by the secondary piece of glassware (part D) that is also cooled by liquid nitrogen.

This isolation method is more preferred as it limits thermal artefact formation compared to other distillation techniques like SDE. This method is also successful at isolating many classes of compounds with little discrimination, including polar, less volatile, and unstable constituents that could be important to many flavor types. Using additional distillation (Vigreux column) and microdistillation (Bemelmans/Kuderna Danish column) techniques, SAFE extracts can be further reduced to increase the analyte concentration within the solvent (Bemelmans, 1979). When a blotter is dipped into a SAFE extract, the odor closely matches the product being studied, which is critical to identifying the key odorants that are representative of the aroma.

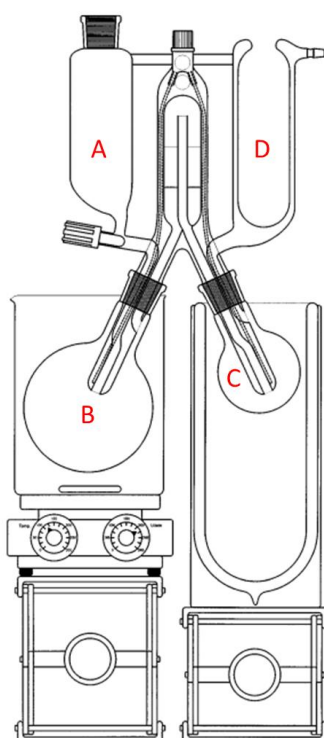


Figure 1.12 An image of a SAFE apparatus (image adapted from Engel, Bahr & Schieberle, 1999).

1.2.4 Static and Dynamic Headspace

Solvent-less headspace techniques have been widely explored in the study of volatile compounds. These sampling techniques can be divided into two main types: dynamic headspace and static headspace. Dynamic headspace (ie purge and trap) incorporates elevated temperatures and purged gas to desorb the volatiles in the headspace of the sample onto a sorbent trap (tenax tube). Advantages of dynamic headspace is the ability to use larger sample sizes to detect lower concentration analytes. Disadvantages include the elevated temperatures, which can lead to degradation and artifact formation of thermally labile compounds, particularly thiols that are often found in Maillard reactions.

Commercialized in the mid-1990s, solid-phase microextraction (SPME) is a static headspace technique that has grown in popularity over the last decade (Vas & Vekey, 2004). Shown in Figure 1.13, SPME is a coated fused silica fiber, which is available in different coating materials depending on which analytes are the focus of isolation and identification. Analytes in the headspace of a sample adsorb onto the fiber and can be directly desorbed into a gas chromatograph (Rouseff, 2002). Overall, SPME is a relatively fast and simple technique, easily automated, and can provide a significant amount of analytical detail with varying volatility and polarity (Werkhoff, Brennecke & Bretschneider, 2002). There are some disadvantages to this technique. As discussed earlier, it becomes difficult to determine if the analytes adsorbed onto the fiber are in representative concentrations above the headspace to accurately define the aroma of the sample. There are many instances of selective adsorption of certain analytes. Authors have noted differences in sensitivity between fibers, artifact formation, discrimination

against polar and very volatile compounds, and how critical it is to find the equilibrium time before extraction (Haberhauer-Troyer, Rosenberg & Grasserbauer, 1999; Pelusio, Nilsson, Montanarella, Tilio, Larsen, Facchetti & Modsen, 1995).

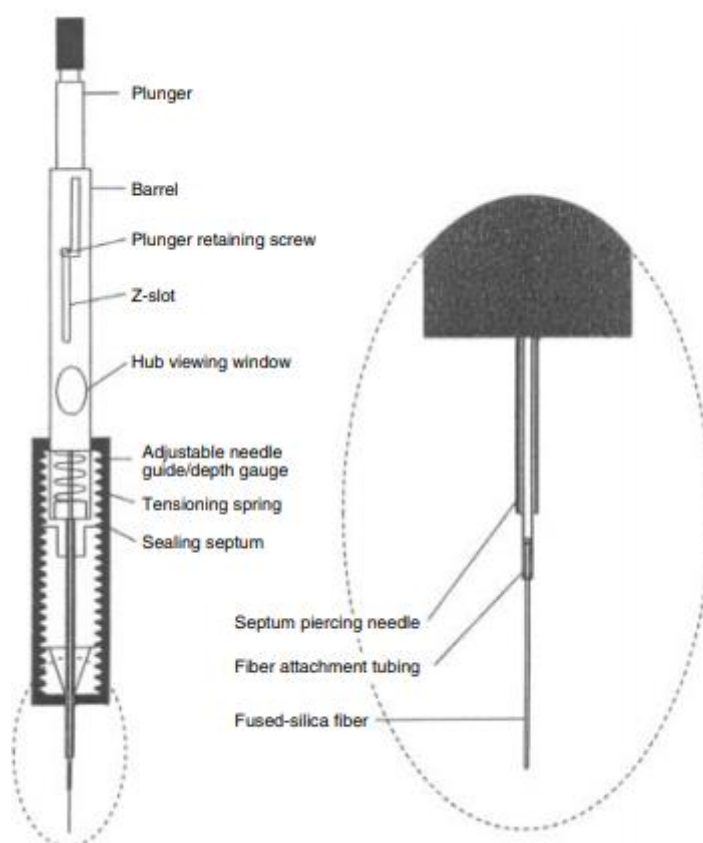


Figure 1.13 An image of solid-phase microextraction (SPME; image adapted from Vas & Vekey, 2004).

Hypothesis and Objectives

2.1 Hypothesis

Over the last fifty years, research on Maillard reactions has dealt predominantly with either simple model systems or complex culinary processes. The next step in our understanding of Maillard reactions is to bridge the chemical and sensory gap between simple and complex model systems. Only a few articles in the literature discuss the reaction of more than one amino acid in the Maillard system. In 1996, Samsudin et al. studied the reaction of leucine and valine with glucose (Samsudin, Rongtao & Said, 1996), while Haleva-Toledo et al. studied the combination of addition of arginine and cysteine on the production of sugar degradation products from glucose and sucrose (Haleva-Toledo, Naim, Zehavi & Rouseff, 1999). More recently, Hou et al. synthesized the Amadori intermediates for both cysteine and glycine to study its reaction with a free amino acid and xylose for the enhancement of meat flavors (Hou, Xie, Zhao, Zhao, Fan, Xiao, Liang & Chen, 2017). The authors measured higher concentrations of volatile sulfur compounds in the reaction of the Amadori intermediate of cysteine and free glycine, compared to the reaction of the Amadori intermediate of glycine and free cysteine.

By adding more than one amino acid to a model Maillard reaction, this research should lead to new discoveries and insights into the competitive reactions and the key odorants formed. This data could provide useful information to reaction chemists and product developers to enhance or control certain compounds in model reactions. In addition, the Strecker aldehyde of arginine has not been successfully isolated and identified in

the Maillard reaction. Based on the mechanisms established for the formation of Strecker aldehydes from other amino acids, a prediction for the structure of the Strecker aldehyde of arginine is shown in Figure 2.1. The Strecker aldehyde could further rearrange to form a pyrrolidinol-like structure under certain conditions. Based on the chemistry and molecular weight of both products, a prediction can be made for the possible MS fragmentation ions produced. This may offer a faster identification when searching the MS data of the arginine reactions described in upcoming sections.

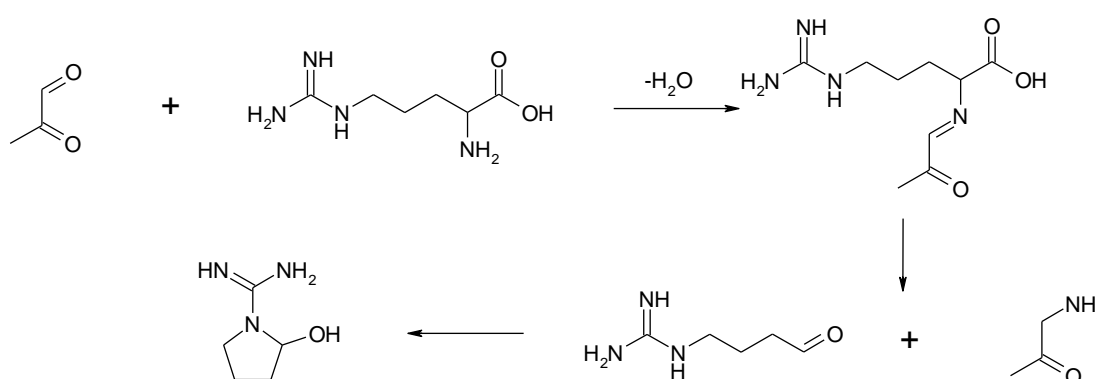


Figure 2.1 Predicted formation of the Strecker aldehyde derived from the reaction of methyl glyoxal and arginine.

Finally, Likens-Nickerson extraction has been the traditional methodology to isolate the aroma compounds from Maillard reactions. The qualitative results in the literature based on this technique could be inaccurate due to the propensity for thermal artifact formation and preferential extraction of hydrophobic compounds. By incorporating liquid-liquid extraction and SAFE, the expectation would be for a more quantitative isolation of the aroma constituents.

2.2 Research Objectives

The objectives for this research are to identify and quantify the key odorants from arginine/cysteine-glucose model studies by gas chromatography-mass spectrometry (GC-MS) and gas chromatography-olfactometry (GC-O). Experimental data will hopefully show that SAFE is a more preferred extraction methodology compared to SDE. Using established literature and predictive modeling, the mechanisms for which several key odorants are formed will be discussed. Finally, a strategy to prove these mechanisms and ideas for supplementary reactions will be briefly discussed.

Experimental

3.1 Materials

The following reagents were purchased from Sigma-Aldrich (St. Louis, MO, USA): L-arginine, L-cysteine, glucose, 3-mercaptopropionic acid, and 2-mercaptopropionic acid. Three molecules were purchased from Enamine (Ukraine): 2-(5-methylpyrazin-2-yl)ethan-1-ol (CAS 142780-03-8); 2-(pyrazin-2-yl)ethan-1-ol (CAS 6705-31-3); 2-(6-methylpyrazin-2-yl)ethan-1-ol (CAS 61892-93-1). Diethyl ether was purchased from Fisher Scientific (Waltham, MA, USA).

3.2 Instruments

The gas chromatography (GC) system consisted of an Agilent 7890A GC (Santa Clara, CA, USA). The apolar capillary column had dimensions of 50 m x 320 μ m x 0.52 mm (Restek RTX-1 F&F) and the polar capillary column was 50 m x 320 μ m x 0.5 mm (Varian CP-Wax 58 FFAP CB column).

The gas chromatography-olfactometry (GC-O) system consisted of an Agilent 6890A GC (Santa Clara, CA, USA). The apolar capillary column had dimensions of 50 m x 320 μ m x 0.52 mm (Restek RTX-1 F&F). An Olfactory Detection Port (ODP; GERSTEL, Inc., Linthicum, MD) was equipped on the GC. Olfactory comments were recorded using Dragon Naturally Speaking, Speech Recognition Software 12.0 (Nuance Communications, Inc., Burlington, MA) in conjunction with the ODP software.

The gas chromatography-mass spectrometry (GC-MS) system consisted of a Waters GCT-Premier orthogonal acceleration time-of-flight (TOF) mass spectrometer (Milford, MA, USA) in electron ionization (EI) mode. The ion source was operated at 150 °C with an electron energy of 70 eV and a trap current of 50 μ A. The temperature of the transfer line was 250 °C. Spectra were acquired between 27 and 400 Da in a time of 0.05 s and a delay of 0.01 s (approximately 20 spectra/s). The apolar capillary column had dimensions of 50 m x 320 μ m x 0.52 mm (Restek RTX-1 F&F) and the polar capillary column was 50 m x 320 μ m x 0.5 mm (Varian CP-Wax 58 FFAP CB column).

The high-performance liquid chromatography (HPLC) system consisted of an Agilent 1100, including an Agilent 1260 Quaternary pump, a diode array detector, and an Agilent 1260 autosampler. HPLC was performed on a Zorbax Eclipse DBX-C8 column (4.6 x 150 mm, 5 μ m, Agilent Part #993967-906).

NMR spectra were recorded on a Bruker Avance 400 MHz spectrometer (Billerica, MA, USA), with 5 mm BBO probes.

3.3 Methods

3.3.1 Preparation of Maillard Reactions

Equimolar ratios of glucose (0.90 g; 5 mmol) and L-arginine (0.87 g; 5 mmol) were added to distilled water (50 mL). An initial pH of 10.4 was measured for the solution.

The pH of the arginine solution was reduced to 7.4 by dropwise addition of 1N HCl and added to 75 mL reaction vessels. The vessels were heated in an oil bath for 1 hour at three different reaction temperatures (100 °C; 130 °C; 160 °C). The same reaction was also carried out at the initial pH of 10.4 with a reaction temperature of 160 °C. Upon completion of the reaction, the vessels were added to an ice bath to cool to room temperature and a second pH measurement was made.

Equimolar ratios of glucose (0.90 g; 5 mmol) and L-cysteine hydrochloride (0.79 g; 5 mmol) were added to distilled water (50 mL). An initial pH of 1.7 was measured for the solution. The pH of the cysteine solution was increased to pH 7.4 by dropwise addition of 2N NaOH and added to 75 mL reaction vessels. The vessels were heated in an oil bath for 1 hour at three different reaction temperatures (100 °C; 130 °C; 160 °C). Upon completion of the reaction, the vessels were added to an ice bath to cool to room temperature and a second pH measurement was made.

Equimolar ratios of glucose (0.90 g; 5 mmol), L-cysteine hydrochloride (0.79 g; 5 mmol), and L-arginine (0.90 g; 5 mmol) were added to distilled water (50 mL). An initial pH of 5.9 was measured for the solution. The pH of the solution was increased to pH 7.4 by dropwise addition of 1N NaOH and added to 75 mL reaction vessels. The vessels were heated in an oil bath for 1 hour at three different reaction temperatures (100 °C; 130 °C; 160 °C). Upon completion of the reaction, the vessels were added to an ice bath to cool to room temperature and a second pH measurement was made.

3.3.2 Liquid-Liquid Extraction of Maillard Reaction

The extraction procedure for all reactions followed the same procedure in Section 3.3.2 and 3.3.3. Once the reaction was cooled to room temperature, each solution was added to a separatory funnel and extracted twice with 25 mL of diethyl ether using an internal standard of octanol at 1 ppm. The extracts were combined, dried over anhydrous sodium sulfate, filtered, and added to a SAFE apparatus for isolation of the volatile compounds.

3.3.3 Solvent Assisted Flavor Evaporation of Maillard Extracts

An image of the SAFE apparatus used in this study is shown in Figure 3.1. The sample was added dropwise into the system, keeping the vacuum below 5×10^{-4} Torr. The frozen extract was allowed to thaw and finally reduced under a gentle stream of nitrogen to 250 μ l.



Figure 3.1 An image of a SAFE setup used to isolate the volatile fraction of the diethyl ether extract.

3.3.4 Steam Distillation Extraction of Maillard Reaction

To compare the extraction effectiveness of SDE to SAFE, a second reaction of cysteine-glucose was charged into a Likens-Nickerson apparatus fitted with a 250 mL reaction vessel, stir bar, and distilled for 1 hour with 50 mL of diethyl ether (1 ppm of octanol as internal standard). The extract was dried over anhydrous sodium sulfate, filtered, and reduced under a gentle stream of nitrogen to 250 μ l.

3.3.5 GC-Analysis of Maillard Extracts

The extract was analyzed on apolar and polar phase columns using an Agilent 7890A gas chromatograph (Santa Clara, CA, USA). The apolar capillary column had dimensions of 50 m x 320 μ m x 0.52 mm (Restek RTX-1 F&F), and the polar capillary column had dimensions of 50 m x 320 μ m x 0.5 mm (Varian CP-Wax 58 FFAP CB column). Samples were introduced to the gas chromatograph (GC) using an autosampler at a volume of 1 μ L with a split ratio of 5:1. The hydrogen carrier gas flow rate was held constant at 2 mL/min, and the temperature program started at an initial temperature of 40 $^{\circ}$ C, then increased 2 $^{\circ}$ C/min up to 250 $^{\circ}$ C with a 10 min hold at 250 $^{\circ}$ C. The end of each apolar and polar column was affixed to a flame ionization detector (FID). The GC was calibrated using a homologous series of C₁-C₁₈ ethyl esters to generate retention index values for the observed peaks. The retention index values were calculated based on previous work by van den Dool and Kratz (Van den Dool & Kratz, 1963), which considers the GC oven temperature program and non-alkane based calibrants, specifically ethyl esters. While this is an industry standard, it is commonly expected to report Kovats retention indices (RI), which are based off calibrations with a homologous series of alkanes. A linear relationship between the ethyl ester values and Kovats RI is found when plotting the measured values for the homologous series of the ethyl esters versus the Kovats values. Based on this relationship the following equation is derived:

$$y = 0.0101x - 3.9494$$

It is with this equation that the Kovats values reported here have been calculated.

3.3.6 GC-MS Analysis of Maillard Extracts

The chromatographic conditions were the same as described for the GC analysis. All data was acquired using a Waters GCT-Premier orthogonal acceleration time-of-flight (TOF) mass spectrometer (Milford, MA, USA) in electron ionization (EI) mode. The ion source was operated at 150 °C with an electron energy of 70 eV and a trap current of 50 μ A. The temperature of the transfer line was 250 °C. Spectra were acquired between 27 and 400 Da in a time of 0.05 s and a delay of 0.01 s (approximately 20 spectra/s). Exact mass spectra were obtained using a single-point lock mass (m/z 218.9856 from perfluorotri-*n*-butylamine) infused into the ion source continuously during the run. Mass spectral library identification was achieved using the data acquired from synthesized or purchased authentic standards. Standard relative retention data was used for confirmation, which was obtained by calibrating the instrument with a homologous series of ethyl esters.

3.3.7 GC-O Analysis of Maillard Extracts

Each extract was analyzed on an apolar 50 m x 320 μ m x 0.5 μ m column (Restek) using an Agilent 6890A GC. All samples were introduced to the GC inlet using an autosampler at a volume of 1 μ L with a 5:1 split ratio. The following parameters remained constant for all samples. The hydrogen carrier gas flow rate was 2 mL/min, and the temperature program started at an initial oven temperature of 40 °C, then increased 6 °C/min up to 80 °C, 4 °C/min up to 150 °C, 2 °C/min up to 200 °C, and finally 10 °C/min up to 310 °C and held for 5 min. In addition, an Olfactory Detection Port (ODP; GERSTEL, Inc., Linthicum, MD) was equipped on the GC. The effluent was split 6:1 (ODP:FID), and the ODP transfer line heated to 225 °C. Olfactory

comments were recorded using Dragon Naturally Speaking, Speech Recognition Software 12.0 (Nuance Communications, Inc., Burlington, MA) in conjunction with the ODP software. The GC was calibrated using a homologous series of C1-C18 ethyl esters to generate index values for the observed peaks and then converted to Kovats values using the aforementioned equation.

3.3.8 NMR Analysis

NMR spectra were recorded at 26.8 °C in deuterated chloroform (containing 0.05% v/v tetramethylsilane) on a Bruker Avance 400 MHz spectrometer (Billerica, MA, USA), with 5 mm BBO probes. ¹H chemical shifts are expressed as parts per million (ppm) with residual chloroform (δ 7.26) or tetramethylsilane (δ 0.00) as a reference and are reported as chemical shift (δ H), relative integral, multiplicity (s = singlet, br = broad, d = doublet, t = triplet, higher multiplicities as e.g. dd = doublet of doublets, m = multiplet); and coupling constants (*J*) reported in Hz.

3.3.9 Measurements of Partition Coefficients by HPLC

To determine the partition coefficient of 2-mercaptopropionic acid and 3-mercaptopropionic acid, a method was developed that followed a procedure according to the Organization for Economic Co-operation and Development (OECD) Guidelines for the Testing of Chemicals no. 117: "Partition Coefficient (n-octanol/water), High Performance Liquid Chromatography (HPLC) Method", April 13, 2004 and the European Economic Community (EEC), EEC Directive 92/69 EEC, Part A, Methods

for the Determination of Physico-Chemical Properties A.8: "Partition Coefficient", EEC Publication no. L383, July 31, 1992. Deviations from OECD Guidelines: no pH measurements were performed. HPLC was performed on a Zorbax Eclipse DBX-C8 column (4.6 x 150 mm, 5 μ m, Agilent Part #993967-906). Ingredients injected onto such a column move along by partitioning between the mobile solvent phase and the hydrocarbon stationary phase. The chemicals are retained in proportion to their hydrocarbon-water partition coefficient, with water-soluble chemicals eluting first and oil-soluble chemicals last. Hence the relationship between the retention time on a C8 column and hydrophobicity can be established. The partition coefficient is calculated from the capacity factor k , given by the expression:

$$k = (t_r - t_0) / t_0$$

where, t_r is the retention time of the test substance, and t_0 is the dead-time or the average time a solvent molecule needs to pass the column. No quantitation is necessary, only accurate retention times.

The partition coefficient of the test substance can be estimated using a computer program calculation method, or where appropriate, by using the ratio of the solubility of the test substance in the pure solvents (see Appendix for additional details).

Results

4.1 Maillard Reaction of Arginine-Glucose

As previously discussed, few studies in the literature have attempted to identify and quantify the volatile compounds produced from the reaction of arginine in the Maillard reaction. Therefore, the focus of this research was to measure the volatile compounds produced from several arginine reactions, including changes in reaction temperature and pH. First, the analytical and sensory data for three reaction temperatures (100 °C, 130 °C, 160 °C) were acquired at the same adjusted pH of 7.4 (initial pH 10.4). There were clear differences in the color at the three different reaction temperatures (see Figure 4.1). At 100 °C, very little aroma was perceived, and no color change was observed. This linked to the analytical data where only a couple trace compounds could be identified. At 130 °C, a weak sweet brown, pretzel-like aroma was detected with a light-yellow color. This temperature yielded slightly higher concentrations of low molecular weight pyrazines (pyrazine; methylpyrazine) along with sugar degradation products (furfural; furfuryl alcohol). Finally, at 160 °C, the pH dropped to 5.2 by the end of the reaction and a more pronounced sweet brown, pretzel-like, nutty aroma was perceived, along with a deeper reddish, brown color. The chromatogram for this reaction yielded a series of alkylpyrazines as well as several furans.

In addition, two arginine-glucose (Arg-Glu) reactions were compared under the same reaction temperature (160 °C) at both pH 7.4 and pH 10.4. The initial pH of the solution of Arg-Glu (before heat treatment) measured 10.4. After the Maillard reaction, the pH

measured 6.8, which represents a significant drop in pH. In contrast, when the initial pH was adjusted to 7.4 before heat treatment, the pH after heat treatment measured 5.2. The differences between initial and final pH of both model systems is significant and will undoubtedly impact sugar fragmentation and the conditions suitable to generate Maillard chemistry. This was certainly observed in both the color changes and the concentration of volatile constituents. As mentioned earlier, a deep reddish, brown color is observed in Figure 4.1 for the reaction at pH 7.4. For the reaction at pH 10.4, the color is significantly darker and appears like balsamic vinegar.



Figure 4.1 Four reactions of Arg-Glu. From left to right: Arg-Glu at 100 °C at pH 7.4; Arg-Glu at 130 °C at pH 7.4; Arg-Glu at 160 °C at pH 7.4; Arg-Glu at 160 °C at pH 10.4.

The analytical data for each of the arginine-glucose reactions can be found in Table 4.1. The total concentration of volatile compounds increased as the temperature and pH of the reaction increased. At pH 7.4, a total of 7.1 mg/mol of pyrazines was measured. At pH 10.4, a total of 207.9 mg/mol of pyrazines was measured. The largest differences were found in the concentration of pyrazine, methylpyrazine, 2,5-dimethylpyrazine and 2,6-dimethylpyrazine. At the higher initial pH, sugar fragmentation is catalyzed more readily under these basic conditions. Sugar degradation products, including glyoxal

and methylglyoxal, react readily with ammonia or the amino group of arginine to form two and three-carbon α -amino fragments, which are the building blocks of substituted alkylpyrazines. For example, the condensation of aminoacetaldehyde and aminoacetone will form 2-methylpyrazine. This compound measured 0.4 mg/mol at pH 7.4 but increases to 105.4 mg/mol at pH 10.4, which is the highest concentration pyrazine derivative in the reaction. This data aligns with previous studies under similar conditions (Huang, Bruechert & Ho, 1989) and suggests a significant increase in the sugar fragmentation and the readily available condensation reactions that occur at higher pH. Due to 2,5-dimethylpyrazine and 2,6-dimethylpyrazine having similar chemistry, neither the polar nor apolar columns could resolve both peaks on a one-dimensional GC column. Therefore, the coeluting peaks are reported as a combination of both compounds in Table 4.1. Similar challenges to resolve these pyrazines have also been noted by other authors (Adams, Polizzi, van Boekel & De Kimpe, 2008). Nonetheless, similar concentration differences to 2-methylpyrazine were observed for the combination of 2,5-dimethylpyrazine and 2,6-dimethylpyrazine at different pH. At pH 7.4, both compounds measured 0.2 mg/mole, while at pH 10.4, both compounds measured 50.1 mg/mol. Even though the ratio of the two dimethylpyrazines was not determined, 2,5-dimethylpyrazine forms from the condensation of two molecules of aminoacetone, while 2,6-dimethylpyrazine forms from the condensation of aminoacetone and 2-aminopropanal (Huang & Ho, 1989).

Additional quantitative differences were observed for the furan-type compounds at each pH. An example includes furaneol (2,5-dimethyl-4-hydroxy-3(2H)-furanone), which is an important aroma compound found in many foods (Wang & Ho, 2008). At pH 10.4, the concentration of furaneol measured 8.3 mg/mol. At pH 7.4, the concentration of

furaneol measured 0.5 mg/mol, which shows a pH dependence on furaneol formation. Numerous studies have investigated the formation pathways of furaneol depending on the reducing sugar and addition of amino acid (Hofmann & Schieberle, 1997; Haleva-Toledo, Naim, Zehavi & Rouseff, 1997; Haleva-Toledo, Naim, Zehavi & Rouseff, 1999; Wang, Juliani, Simon & Ho, 2009). Glucose, a hexose sugar, generates lower concentrations of furaneol compared to rhamnose, a 6-deoxyhexose sugar (Hofmann & Schieberle, 1997). The data from the Arg-Glu reaction suggests that the major formation pathway of furaneol is through the Cannizzaro reaction of methyl glyoxal, which requires basic conditions.

A compound with high toxicological risk is 5-hydroxymethylfurfural (5HMF). This compound is formed from the intermediate 3-deoxyglucosone, which is derived from the 1,2-enolization and dehydration of glucose (Lee & Nagy, 1990). 5HMF (18.6 mg/mol) was only detected at pH 7.4, which aligns with other research in the literature (Gökmen, Açar, Köksel, & Açar, 2007) and demonstrates the preferential 1,2-enolization pathway at lower pH. In 1999, Haleva-Toledo et al. studied the effect of the addition of arginine on the production of 5HMF from glucose under acidic conditions (Haleva-Toledo, Naim, Zehavi & Rouseff, 1999). The concentration of 5HMF increased in the presence of arginine. The opposite trend was found with furfuryl alcohol (currently GRAS status) where high concentrations were found at pH 10.4 (34.7 mg/mol) compared to the reaction at pH 7.4 (1.6 mg/mol). This shows that the major precursors to furfuryl alcohol, likely 3-deoxyaldoketose or 2-deoxyribose (Brands & van Boekel, 2001), are generated at higher pH.

A final observation from the analysis of the Arg-Glu reaction relates to the identification of 2-aminophenol (8.1 mg/mol at pH 7.4; 2.7 mg/mol at pH 10.4). Scarcely described in Maillard-type literature studies, the formation of 2-aminophenol could be derived from the intermediate benzene-1,2-diol, which was detected in the reaction at pH 10.4. Benzene-1,2-diol, a hydroxylated benzene, can be generated from glucose (Haffenden & Yaylayan, 2005). Further research is required to support this hypothesis.

Table 4.1 The analytical data from the Arg-Glu reactions.

Compound	OV1 (Kovats)	Arg-Glu (100 °C) SAFE pH 7.4*	Arg-Glu (130 °C) SAFE pH 7.4*	Arg-Glu (160 °C) SAFE pH 7.4*	Arg-Glu (160 °C) SAFE pH 10.4*
pyrazines					
pyrazine	716	0.06	0.15	4.79	24.18
2-methylpyrazine	804	nd	0.01	0.42	105.40
2,6- + 2,5-dimethylpyrazine	891	nd	nd	0.21	50.10
2-ethylpyrazine	898	nd	nd	0.25	6.00
2,3-dimethylpyrazine	898	nd	nd	0.08	4.08
2-vinylpyrazine	928	nd	0.01	0.56	3.32
2-ethyl-6-methylpyrazine	978	nd	nd	nd	3.73
2-ethyl-5-methylpyrazine	981	nd	nd	nd	2.02
2,3,5-trimethylpyrazine	988	nd	nd	nd	6.21
2-methyl-5-vinylpyrazine	998	nd	Nd	nd	2.12
quinoxaline	1173	nd	Nd	0.78	0.76
<i>total pyrazines</i>		0.06	0.17	7.09	207.91
furans/pyrans					
furfural	809	nd	0.49	2.96	0.63
furfuryl alcohol	828	nd	0.10	1.57	34.65
2-acetylfuran	890	0.06	0.01	0.52	nd
5-methylfurfural	939	nd	nd	0.57	nd
5-methyl-2-furanmethanol	947	nd	nd	nd	2.43
furaneol	1030	nd	nd	0.53	8.30
5-hydroxy-5,6-dihydromaltol	1116	0.01	0.13	3.39	5.25
5-hydroxymethylfurfural	1177	nd	0.04	18.58	nd
<i>total furans/pyrans</i>		0.07	0.78	28.12	51.27
misc.					
1-hydroxypropan-2-one	622	nd	nd	0.84	16.08
acetoin	680	nd	nd	0.18	2.06
cyclopentanone	763	nd	nd	nd	nd
cyclohexan-1,2-dione	974	nd	0.39	nd	nd
cyclotene	997	nd	nd	1.05	8.58
2-aminophenol	1177	nd	nd	8.11	2.70
benzene-1,2-diol	1168	nd	nd	nd	7.74
acetaldehyde	485	0.30	0.44	0.14	0.26

nd – not detected; * Data reported in mg/mol of arginine from the average of two runs.

Based on the proposed mechanism in Figure 2.1 of the Hypothesis section, there was no evidence from the MS data that the Strecker aldehyde of arginine was generated in any of the four Arg-Glu reactions. Perhaps the positively charged guanidine group or the rearranged pyrrolidinol-like compound would not be extracted and/or detected under the described experimental conditions.

4.1.1 Identification of Hydroxyethyl Pyrazines

GC-Olfactometry was performed to identify the aroma-active compounds from the Arg-Glu reactions. Odor comments were recorded at the end of the ODP using the Dragon software to record each odor comment. Even though there were similar odorants perceived in both reactions at pH 7.4 and 10.4, the intensity of those odorants (“nutty, burnt, chocolate, pyrazinic”) was significantly higher in the reaction at pH 10.4 (data not shown). There were two separate odor comments from this reaction that were not immediately linked to a known MS library spectrum. Both peaks in the chromatogram were low in concentration (<0.1 mg/mol) but were described as “chocolate, pyrazinic, nutty” and “nutty, popcorn”.

The MS spectra for both peaks are shown in Figure 4.2. Based on exact mass measurements from a TOF mass spectrometer and elemental composition of the molecular ion and associated fragments, two structures, 2-(pyrazin-2-yl)ethan-1-ol and 2-(5-methylpyrazin-2-yl)ethan-1-ol, were postulated and synthesized. Along with 2-(6-methylpyrazin-2-yl)ethan-1-ol, the vendor synthesized standards were confirmed as the unknowns found in the Arg-Glu reaction. These three compounds are scarcely reported

in the literature and still yet to be reported in a natural product. Shu tentatively identified 2-(pyrazin-2-yl)ethan-1-ol in the thermal reaction of glucosamine (Shu, 1998), and later identified 2-(6-methylpyrazin-2-yl)ethan-1-ol in the reaction of inulin/asparagine and fructose/asparagine (Shu, 1998b).

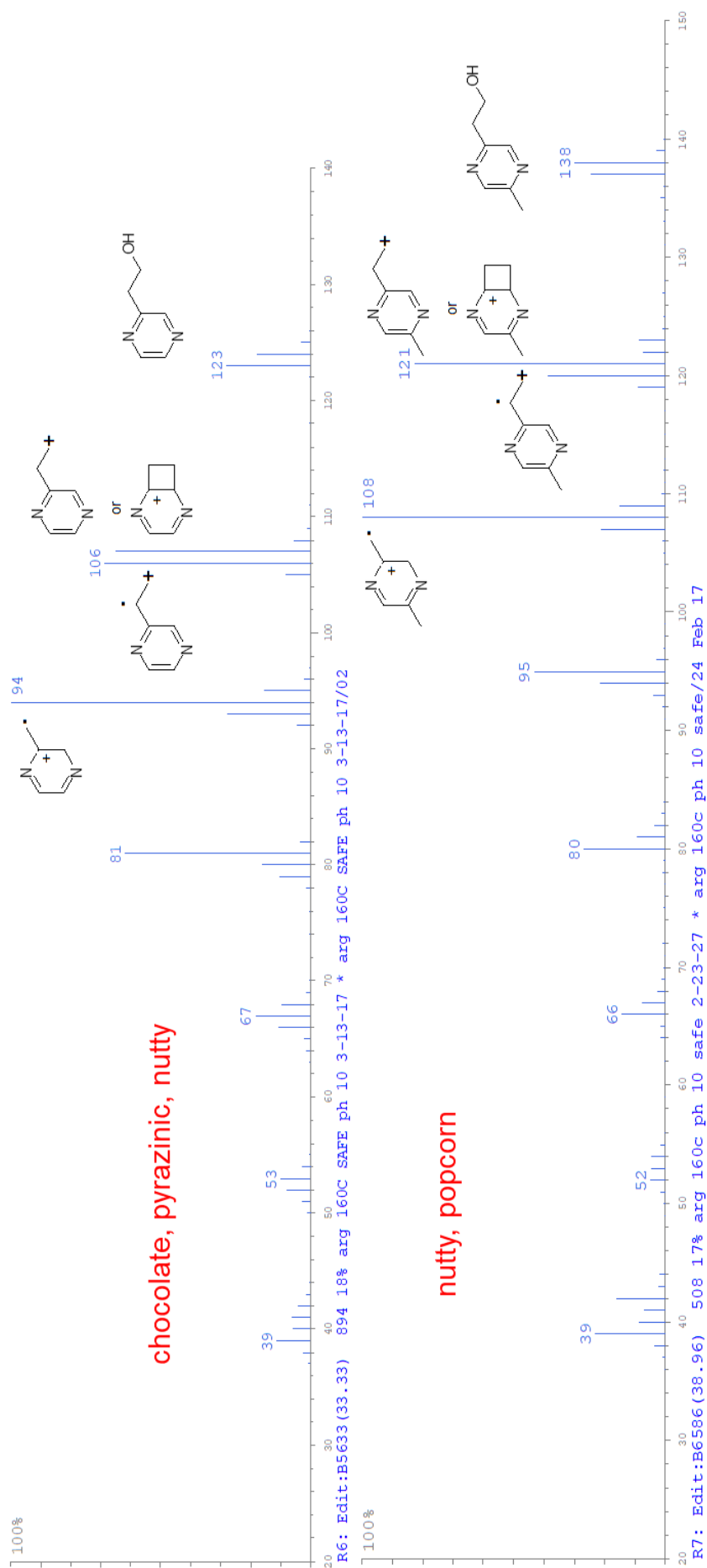
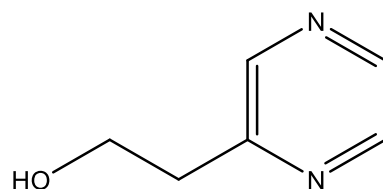
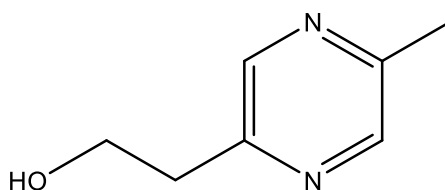


Figure 4.2 The spectra and predicted fragmentation pattern of (A) 2-(pyrazin-2-yl)ethan-1-ol and (B) 2-(5-methylpyrazin-2-yl)ethan-1-ol based on the elemental composition of the molecular ion and associated fragments from exact mass measurements.

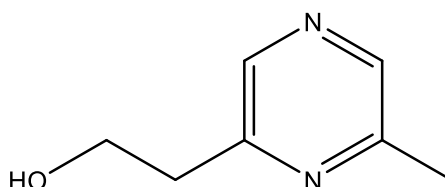
The structure, NMR data, MS data, and odor descriptors for each of the three hydroxyethyl pyrazines are described below:



2-(pyrazin-2-yl)ethan-1-ol (CAS 6705-31-3): ¹H NMR (400 MHz, CHLOROFORM-d) Shift: 8.51 (d, J= 1.4 Hz, 1H), 8.49 (dd, J=2.6, 1.4 Hz, 1H), 8.45 (d, J=2.6 Hz, 1H), 4.06 (t, J=5.7 Hz, 2H), 3.07 (t, J=5.7 Hz, 2H). EI-MS: 124 (17, M⁺), 94 (100), 81 (75), 106 (64), 107 (60), 93 (28), 67 (22), 123 (22), 80 (20), 39 (17). FID (Kovats): 1127 (OV1); 1891 (CBW). Odor descriptors from blotter evaluation of 2-(pyrazin-2-yl)ethan-1-ol diluted 1% in ethanol: nutty, pyrazinic, stale, chocolate.



2-(5-methylpyrazin-2-yl)ethan-1-ol (CAS 142780-03-8): ¹H NMR (400 MHz, CHLOROFORM-d) Shift: 8.37 (s, 1H), 8.35 (s, 1H), 4.03 (t, J= 5.6 Hz, 2H), 3.02 (t, J=5.6 Hz, 2H), 2.54 (s, 3H). EI-MS: 138 (38, M⁺), 108 (100), 121 (70), 95 (49), 107 (39), 120 (38), 80 (28), 39 (20), 109 (19), 137 (18). FID (Kovats): 1211 (OV1); 1928 (CBW). Odor descriptors from blotter evaluation of 2-(5-methylpyrazin-2-yl)ethan-1-ol diluted 1% in ethanol: nutty, chocolate, pyrazinic, burnt.

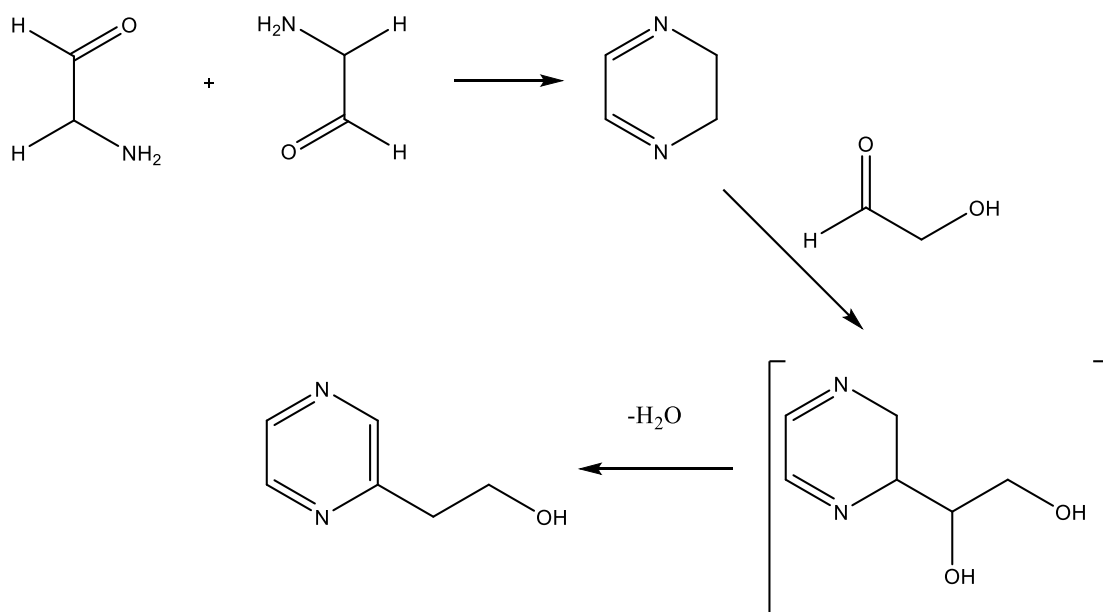
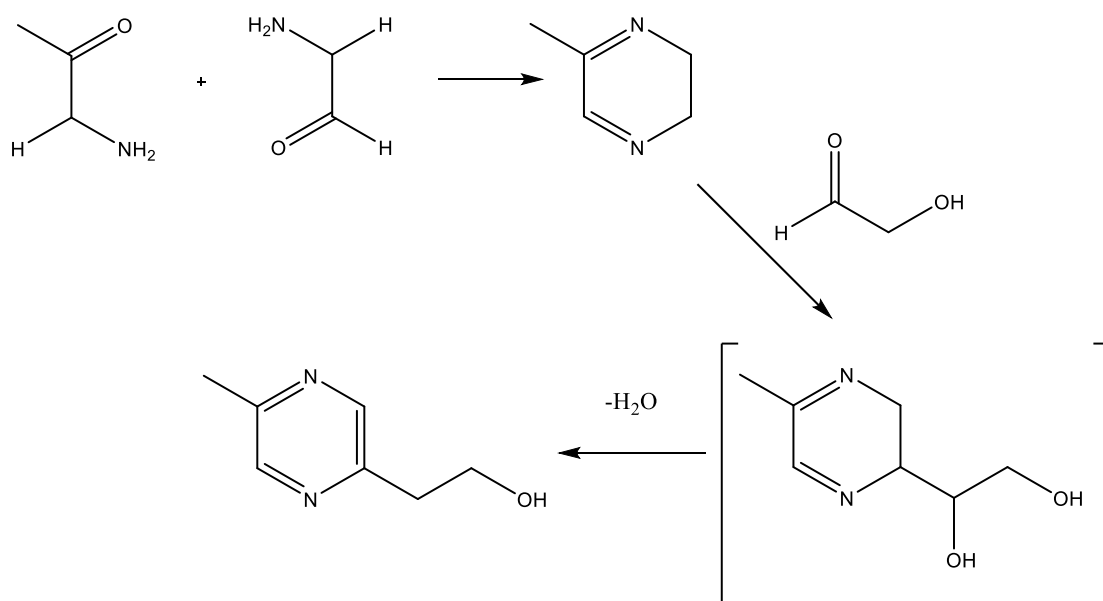


2-(6-methylpyrazin-2-yl)ethan-1-ol (CAS 61892-93-1): ¹H NMR (400 MHz, CHLOROFORM-d) Shift: 8.35 (s, 1H), 8.30 (s, 1H), 4.05 (t, J= 5.6 Hz, 2H), 3.03 (t, J= 5.6 Hz, 2H), 2.56 (s, 3H). EI-MS: 138 (38, M⁺), 108 (100), 121 (79), 95 (41), 120 (39), 107 (25), 137 (24), 94 (23), 109 (19), 39 (19). FID (Kovats): 1205 (OV1); 1917 (CBW). Odor descriptors from blotter evaluation of 2-(6-methylpyrazin-2-yl)ethan-1-ol diluted 1% in ethanol: nutty, burnt, chocolate, pyrazinic.

4.1.2 Proposed Mechanism of Formation of Hydroxyethyl Pyrazines

A couple mechanisms are possible to describe the formation of hydroxyethyl pyrazines. Shown in Figure 4.3, one proposal starts with two equivalents of aminoacetaldehyde to form dihydropyrazine. Glycoaldehyde, one of the most reactive sugar fragmentation

products (Nursten, 2005), would then react with the dihydropyrazine intermediate to form an unstable diol. Dehydration followed by the migration of the double bond into the ring forms a more stable hydroxyethyl pyrazine.

A**B**

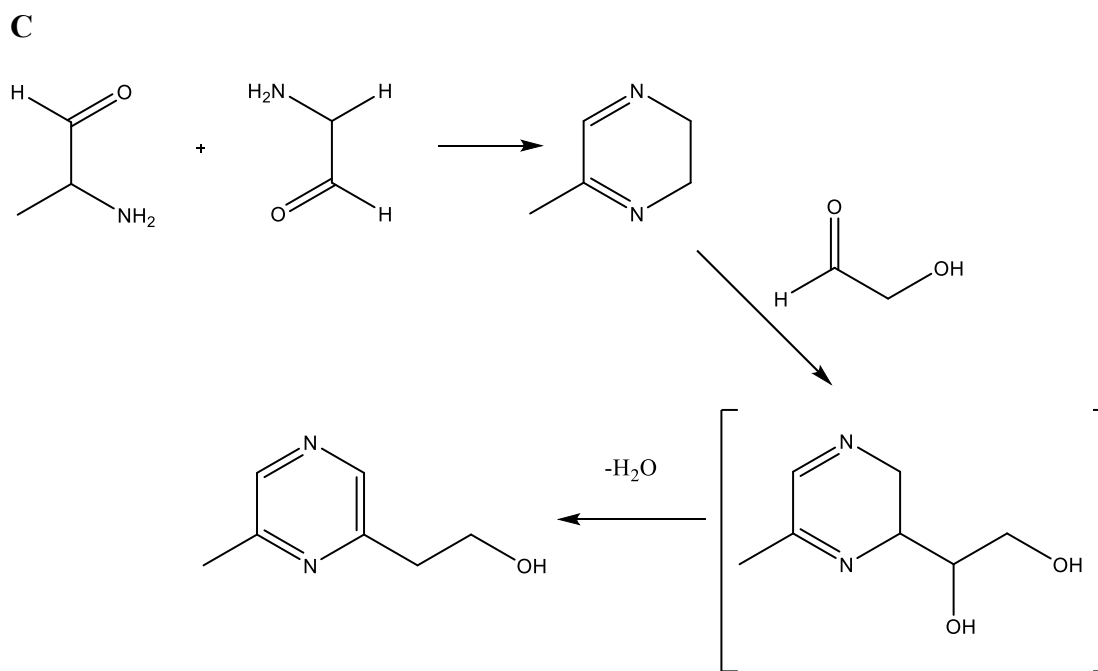


Figure 4.3 Proposed formation of (A) 2-(pyrazin-2-yl)ethan-1-ol; (B) 2-(5-methylpyrazin-2-yl)ethan-1-ol; and (C) 2-(6-methylpyrazin-2-yl)ethan-1-ol.

All three hydroxyethyl pyrazines were identified from an alkaline extraction of a thermal reaction of asparagine-glucose by Bohnenstengel & Baltes (Bohnenstengel & Baltes, 1992). The authors proposed a second possible mechanism for the generation of hydroxyethyl pyrazines whereby the reaction of glyoxal (or methylglyoxal) with the Amadori product of glucose would form 4-(2-pyrazinyl)-1,2,3-trihydroxybutane. Additional oxidation and retro-aldol steps would lead to the formation of the respective hydroxyethyl pyrazines.

Vinylpyrazines are also prevalent in Maillard reactions and often described as green, burnt, nutty, and coffee-like in aroma. In addition, 2-methyl-5-vinylpyrazine (CAS 13925-08-1; FEMA 3211) is registered for flavor use. It is plausible that hydroxyethyl

pyrazines, based on the mechanism described above, act as the intermediates by which water elimination leads to the formation of vinylpyrazines as shown in Figure 4.4.

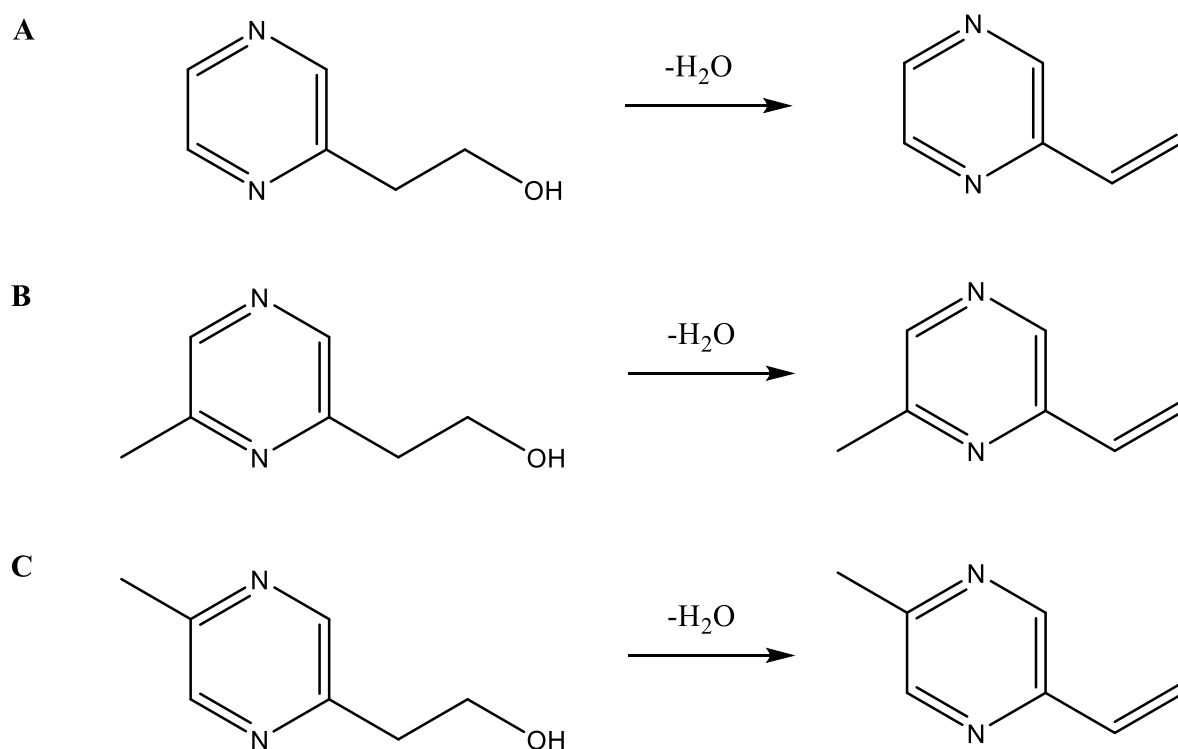


Figure 4.4 Proposed formation of (A) 2-vinylpyrazine (CAS 4177-16-6); (B) 2-methyl-6-vinylpyrazine (CAS 13925-09-6); and (C) 2-methyl-5-vinylpyrazine (CAS 13925-08-1) by water elimination of the respective hydroxyethyl pyrazine.

4.2 Maillard Reaction of Cysteine-Glucose

As discussed in the Introduction, cysteine has been studied extensively in the literature as a sulfur-containing amino acid in the Maillard reaction. Nonetheless, data on the Maillard reaction of Cys-Glu was acquired mainly as a baseline point of reference to compare to arginine/cysteine-glucose (Arg/Cys-Glu) reactions in the next section. The

analytical and sensory data of the Cys-Glu model system were acquired at two reaction temperatures (130 °C; 160 °C) at an adjusted pH of 7.4 (initial pH 1.7). At 130 °C, there was very little color change (slight yellow hue) to the final solution (see Figure 4.5). There was a medium intensity aroma of roasted, meaty notes which was attributed to low concentrations of thiol compounds, including 1-mercaptopropan-2-one and 3-mercaptobutan-2-one. At 160 °C, the pH had dropped to 4.4 by the end of the reaction and the solution was orange in color with a strong aroma of roasted meat and savory notes. By comparing data from the literature, it is evident that the reaction at pH greater than seven is less vigorous compared to reactions closer to the isoelectric point (pH 5.1) of cysteine (Shu, Mookherjee & Ho, 1985).



Figure 4.5 Two reactions of Cys-Glu. From left to right: Cys-Glu at 130 °C at pH 7.4; Cys-Glu at 160 °C at pH 7.4.

The data for the Cys-Glu reactions are presented in Table 4.2. In contrast to the Arg-Glu reaction, the generation of pyrazines in the Cys-Glu reaction at pH 7.4 was considerably lower by SAFE: 1.6 mg/mol in Cys-Glu compared to 7.1 mg/mol in Arg-Glu. This data differed from similar reactions in the literature. For example, Zhang & Ho measured 117.6 mg/mol of total pyrazines from the reaction of Cys-Glu at pH 7.5

(Zhang & Ho, 1991). The temperature of the reaction was slightly higher (180 °C), but the authors incorporated SDE for the isolation of the volatiles. The different extraction methodologies will be discussed in the next section as a possible reason for the inconsistencies in data.

The aroma contribution of each pyrazine of the Cys-Glu reaction were studied by GC-O and compared to the data generated from the Arg-Glu reaction. Results from the Cys-Glu extracts produced very few aromas that were described as ‘nutty, burnt, pyrazinic’ (data not shown). Instead, the dominant odorants from the GC-O smell out of the Cys-Glu extract were instead ‘sulfurous, coffee, roasted, and tropical’. The major constituents linked to these aroms were thiols, including many reported in Table 4.2. Two mercapto acids, 2-mercaptopropionic acid (185.2 mg/mol) and 3-mercaptopropionic acid (97.4 mg/mol), were found at the highest concentrations in the reaction. The formation and physico-chemical properties of these mercapto acids will be discussed in more detail in latter sections. This agrees with previously published GC-O data from Maillard reactions involving cysteine where the most intense odorants were linked to sulfurs or furans (Hofmann & Schieberle, 1998). These compounds, along with other thiol compounds, are extremely potent odorants in foods. For example, 2-methylfuran-3-thiol (CAS 28588-74-1), a key odorant found in meat (Kerschler & Grosch, 1998) and chicken (Farkas, Sadecka, Kovac, Siegmund, Leitner & Pfannhauser, 1997), measured one of the lowest odor thresholds ever recorded, between 0.0000025-0.00001 parts per billion (ppb) in air (Gasser & Grosch, 1990). Even at low concentration of 0.4 mg/mol in the Cys-Glu model reaction, 2-methylfuran-3-thiol can significantly affect the aroma profile as also shown in the literature (Hofmann & Schieberle, 1997). In 2005, de Roos et al. quantified several high impact

thiols from the reaction of cysteine with different carbonyl compounds (de Roos, Wolswinkel & Sipma, 2005). Albeit under different reaction conditions (pH 5.0; open system), the authors found that the Cys-Glu reaction produced significantly lower concentrations of 2-methylfuran-3-thiol, fufuryl mercaptan, 3-mercaptopentan-2-one, and 2-mercaptopentan-3-one, compared to the cysteine-ribose, cysteine-xylose, and cysteine-norfuraneol model systems.

Two less common thiophenones were also identified and quantified in the Cys-Glu reaction at 160 °C: 2,5-dimethyl-4-hydroxy-3(2H)-thiophenone (DMHT; CAS 26494-10-0; 7.5 mg/mol) and 2,5-dimethyl-2,4-dihydroxy-3(2H)-thiophenone (DMDHT; CAS 96504-28-8; 5.7 mg/mol) (see Figure 4.6).

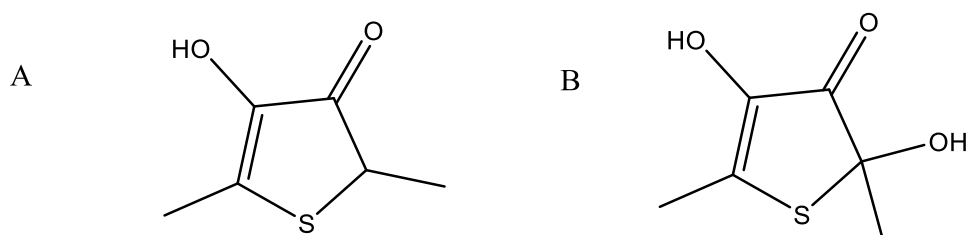


Figure 4.6 The structures of (A) 2,5-dimethyl-4-hydroxy-3(2H)-thiophenone (DMHT) and (B) 2,5-dimethyl-2,4-dihydroxy-3(2H)-thiophenone (DMDHT).

Previously identified in yeasts extracts (Munch, Hofmann & Schieberle, 1997), DMHT has been also identified in Maillard reactions of cysteine-furaneol (Shu, Hagedorn & Ho, 1986; Shu & Ho, 1988; Zheng, Brown, Ledig, Mussinan & Ho, 1997), cysteine-glucose (Tressl, Helak, Martin & Kersten, 1989; Hofmann & Schieberle, 1997), and cystine-furaneol (Shu, Hagedorn, Mookherjee & Ho, 1985). DMDHT has been

identified in soy sauce (Satoh, Nomi, Yamada, Takenaka, Ono & Murata, 2011) and garlic (Hwang, Woo, Kim, Hong, Hwang, Lee & Jeong, 2007; Molina-Calle, Sanchez de Medina, Priego-Capote, & Luque de Castro, 2017), as well as in Maillard reactions of cysteine-furaneol (Shu, Hagedorn & Ho, 1986; Shu & Ho, 1988), cysteine-glucose (Tressl, Helak, Martin & Kersten, 1989), and cystine-furaneol (Shu, Hagedorn, Mookherjee & Ho, 1985). Also known as thiacremonone, DMDHT has been explored recently for its anti-oxidant and anti-inflammatory responses in animal studies (Yun, Jin, Park, Hwang, Jeong, Kim, Jung, Oh, Hwang, Han & Hong, 2016). Described as possessing a pot roast-like aroma, DMHT and DMDHT were reported in the Maillard reactions referenced above at low pH (2-6) and higher temperatures (130-160 °C). The model systems suggest that water elimination from glucose at pH 5-7 will yield 3,4-dihydroxy-3-hexene-2,5-dione (CAS 10153-61-4), which would further react with hydrogen sulfide to form DMHT and DMDHT in a ratio of 10:1 (Tressl, Helak, Martin & Kersten, 1989). Another possible mechanism for the formation of DMHT could be through the hydrolysis of furaneol and subsequent addition of hydrogen sulfide and loss of water.

Table 4.2 The analytical data from the Cys-Glu reactions at two different reaction temperatures.

Compound	OV1 (Kovats)	Cys-Glu (130 °C) SAFE pH 7.4*	Cys-Glu (160 °C) SAFE pH 7.4*
pyrazines			
pyrazine	716	nd	0.07
2-methylpyrazine	804	nd	0.94
2,6- + 2,5-dimethylpyrazine	891	nd	0.12
2-ethylpyrazine	898	nd	0.33
2,3-dimethylpyrazine	898	nd	0.16
2-vinylpyrazine	928	nd	nd
2-ethyl-6-methylpyrazine	978	nd	nd
2-ethyl-5-methylpyrazine	981	nd	nd
2,3,5-trimethylpyrazine	988	nd	nd
2-methyl-5-vinylpyrazine	998	nd	nd
quinoxaline	1173	nd	nd
<i>total pyrazines</i>		0.00	1.61
furans/pyrans			
furfural	809	nd	nd
furfuryl alcohol	828	nd	7.14
2-acetylfuran	890	nd	1.74
5-methylfurfural	939	nd	0.91
5-methyl-2-furanmethanol	947	nd	0.66
furaneol	1030	nd	2.63
5-hydroxy-5,6-dihydromaltol	1116	0.14	5.20
5-hydroxymethylfurfural	1177	nd	nd
<i>total furans/pyrans</i>		0.14	18.29
thiophenes			
thiophene	647	nd	0.50
2-methylthiophene	757	nd	0.16
2,5-dimethylthiophene	861	nd	0.18
2-ethylthiophene	852	nd	nd
2-formylthiophene	975	nd	1.79
2-acetylthiophene	1074	nd	0.33
2-formyl-4-methylthiophene	1091	nd	4.92
tetrahydrothiophen-3-one	920	nd	1.90
3-thiophenethiol	950	0.01	5.89

2-methyltetrahydrothiophen-3-one	958	nd	1.02
3-mercapto-2-methylthiophene	1054	0.02	2.04
2,5-dimethyl-4-hydroxy-3(2h)-thiophenone	1134	0.07	7.53
thieno[3.2.b]thiophene	1176	nd	1.39
2,5-dimethyl-2,4-dihydroxy-3(2h)-thiophenone	1223	0.07	5.72
<i>total thiophenes</i>		0.16	33.38
misc. sulfurs			
methyl mercaptan	484	nd	0.00
1,1-ethanedithiol	715	nd	0.14
2-mercaptoethanol	769	nd	0.12
1-mercaptopropan-2-one	749	0.04	3.97
3-mercaptoputan-2-one	791	0.02	9.21
1,2-ethanedithiol	801	nd	0.41
1-mercaptoputan-3-one	850	nd	0.36
1-mercaptoputan-2-one	852	nd	0.76
2-methylfuran-3-thiol	853	nd	0.43
3-mercaptopentan-2-one	881	nd	0.80
2-mercaptopentan-3-one	886	nd	1.00
furfuryl mercaptan	895	nd	0.33
2-(1-mercaptoethyl)-furan	932	nd	0.47
5-methyl-2-furanmethanethiol	994	nd	1.21
2-mercaptopropionic acid	985	nd	185.24
3-mercaptopropionic acid	998	0.01	97.38
3,5-dimethyl-1,2,4-trithiolane isomer i	1112	nd	1.31
3,5-dimethyl-1,2,4-trithiolane isomer ii	1119	nd	0.60
1,2-dithian-4-one	1124	nd	2.21
5-acetyl-2,3-dihydro-1,4-thiazine	1322	nd	nd
<i>total misc sulfurs</i>		0.08	305.95
misc.			
1-hydroxypropan-2-one	622	nd	0.29
acetoin	680	nd	0.95
cyclopentanone	763	nd	0.71
cyclohexan-1,2-dione	974	nd	nd
cyclotene	997	nd	nd
2-aminophenol	1177	nd	nd
benzene-1,2-diol	1168	nd	nd
acetaldehyde	485	0.08	0.06

nd – not detected; * Data reported in mg/mol of cysteine from the average of two runs.

As discussed in the previous section, 5HMF was identified at high concentrations in the Arg-Glu reaction at pH 7.4. However, in the Cys-Glu reaction, there was no detected

levels of 5HMF at this pH. This aligns with previous reports by Haleva-Toledo et al. who demonstrated that the addition of cysteine in the reaction with glucose (with and without arginine) significantly reduced the concentration of 5HMF (Haleva-Toledo, Naim, Zehavi & Rouseff, 1999). Also, research by Tai & Ho did not detect 5HMF in the reaction of glutathione, a cysteine-containing tripeptide, at pH 6.0 and 8.0 (Tai & Ho, 1998). These results demonstrate the competitive blocking mechanism of the thiol group of cysteine during the initial Maillard stages of amine-carbonyl reactions (Friedman & Molnar-Perl, 1990).

4.2.1 Comparison of SAFE and SDE in Cysteine-Glucose Reaction

Another objective within the research dealt with investigating the effectiveness of two commonly used extraction techniques, steam distillation extraction (SDE) and solvent assisted flavor evaporation (SAFE), in the analysis of the volatile constituents in Maillard reactions. While comparing several literature references that implemented different extraction procedures on Maillard reactions, it became evident of the wide ranging and conflicting data, especially for the Cys-Glu reaction. The analytical data comparing the chemical constituents of the Cys-Glu reaction by SDE and SAFE in the study are shown in Table 4.3. Notable differences were measured when comparing the levels of total pyrazines (1.6 mg/mol by SAFE; 6.8 mg/mol by SDE), total furans/pyrans (18.3 mg/mol by SAFE; 30.8 mg/mol by SDE), and total thiophenes (33.4 mg/mol by SAFE, 73.4 mg/mol by SDE). Thermal processing inherent in the SDE appears to generate additional concentrations of volatile compounds either from previously unreacted cysteine and glucose or from condensation intermediates (eg

Amadori products). There is also the possibility of artifact formation where certain existing volatiles from the Maillard reaction are further degrading into smaller molecular weight molecules. The increase in concentration of acetaldehyde from SDE (14.9 mg/mol) can be generated from glucose or the decarboxylation of cysteine during the extended thermal treatment.

Table 4.3 The analytical data from SDE and SAFE extracts of the Cys-Glu reactions.

Compound	OV1 (Kovats)	Cys-Glu (160 °C) SAFE pH 7.4*	Cys-Glu (160 °C) SDE pH 7.4*
pyrazines			
pyrazine	716	0.07	0.42
2-methylpyrazine	804	0.94	4.35
2,6- + 2,5-dimethylpyrazine	891	0.12	0.70
2-ethylpyrazine	898	0.33	0.86
2,3-dimethylpyrazine	898	0.16	0.42
2-vinylpyrazine	928	nd	nd
2-ethyl-6-methylpyrazine	978	nd	nd
2-ethyl-5-methylpyrazine	981	nd	nd
2,3,5-trimethylpyrazine	988	nd	nd
2-methyl-5-vinylpyrazine	998	nd	nd
quinoxaline	1173	nd	nd
<i>total pyrazines</i>		1.61	6.75
furans/pyrans			
furfural	809	nd	0.25
furfuryl alcohol	828	7.14	10.92
2-acetylfuran	890	1.74	4.82
5-methylfurfural	939	0.91	12.80
5-methyl-2-furanmethanol	947	0.66	1.65
furaneol	1030	2.63	nd
5-hydroxy-5,6-dihydromaltol	1116	5.20	0.35
5-hydroxymethylfurfural	1177	nd	nd
<i>total furans/pyrans</i>		18.29	30.78
thiophenes			
thiophene	647	0.50	2.89
2-methylthiophene	757	0.16	1.87
2,5-dimethylthiophene	861	0.18	1.10
2-ethylthiophene	852	nd	3.49
2-formylthiophene	975	1.79	2.26
2-acetylthiophene	1074	0.33	2.02
2-formyl-4-methylthiophene	1091	4.92	8.28
tetrahydrothiophen-3-one	920	1.90	8.69
3-thiophenethiol	950	5.89	14.47
2-methyltetrahydrothiophen-3-one	958	1.02	1.83
3-mercapto-2-methylthiophene	1054	2.04	8.41

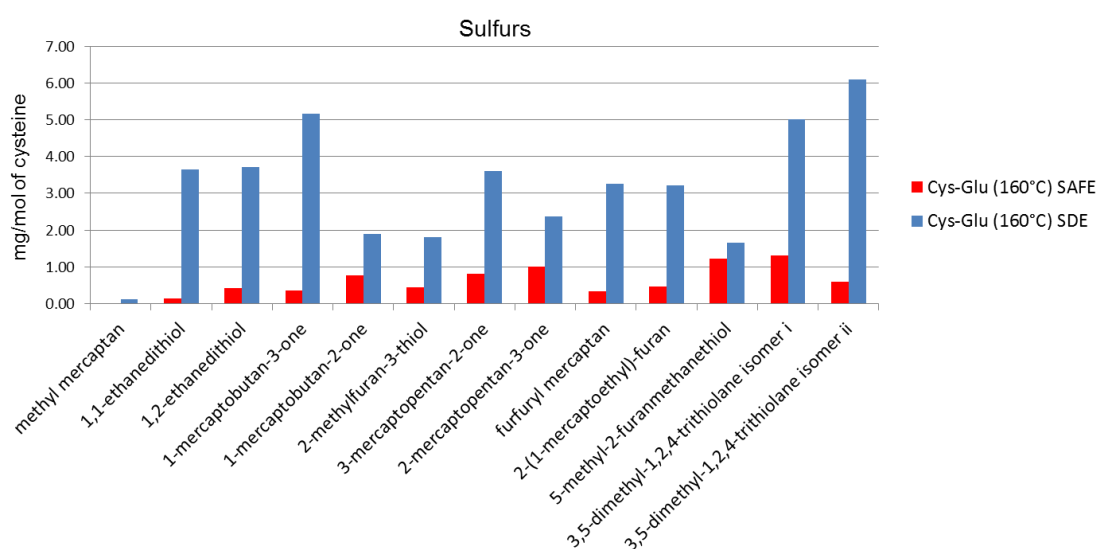
2,5-dimethyl-4-hydroxy-3(2h)-thiophenone	1134	7.53	9.68
thieno[3.2.b]thiophene	1176	1.39	4.96
2,5-dimethyl-2,4-dihydroxy-3(2h)-thiophenone	1223	5.72	3.43
<i>total thiophenes</i>		33.38	73.37
misc. sulfurs			
methyl mercaptan	484	nd	0.13
1,1-ethanedithiol	715	0.14	3.65
2-mercaptoethanol	769	0.12	0.66
1-mercaptopropan-2-one	749	3.97	21.49
3-mercaptoputan-2-one	791	9.21	24.71
1,2-ethanedithiol	801	0.41	3.71
1-mercaptoputan-3-one	850	0.36	5.17
1-mercaptoputan-2-one	852	0.76	1.88
2-methylfuran-3-thiol	853	0.43	1.81
3-mercaptopentan-2-one	881	0.80	3.61
2-mercaptopentan-3-one	886	1.00	2.37
furfuryl mercaptan	895	0.33	3.25
2-(1-mercaptoethyl)-furan	932	0.47	3.21
5-methyl-2-furanmethanethiol	994	1.21	1.65
2-mercaptopropionic acid	985	185.24	nd
3-mercaptopropionic acid	998	97.38	nd
3,5-dimethyl-1,2,4-trithiolane isomer i	1112	1.31	5.02
3,5-dimethyl-1,2,4-trithiolane isomer ii	1119	0.60	6.09
1,2-dithian-4-one	1124	2.21	12.65
5-acetyl-2,3-dihydro-1,4-thiazine	1322	nd	nd
<i>total misc sulfurs</i>		305.95	101.04
misc.			
1-hydroxypropan-2-one	622	0.29	0.17
acetoin	680	0.95	1.73
cyclopentanone	763	0.71	1.94
cyclohexan-1,2-dione	974	nd	nd
cyclotene	997	nd	nd
2-aminophenol	1177	nd	nd
benzene-1,2-diol	1168	nd	nd
acetaldehyde	485	0.06	14.92

nd – not detected; * Data reported in mg/mol of cysteine from the average of two runs.

Additional chemical differences were observed from the concentration of sulfur compounds. Table 4.4 compares several high impact, low concentration sulfur compounds. Even though the concentrations of these sulfur compounds are low, many

of these compounds have odor thresholds in the ng/L level. Therefore, even small differences between the concentration in the SAFE or SDE extracts can significantly affect the aroma profile. The data again suggests thermal artifact formation during the isolation of volatile sulfur compounds by SDE.

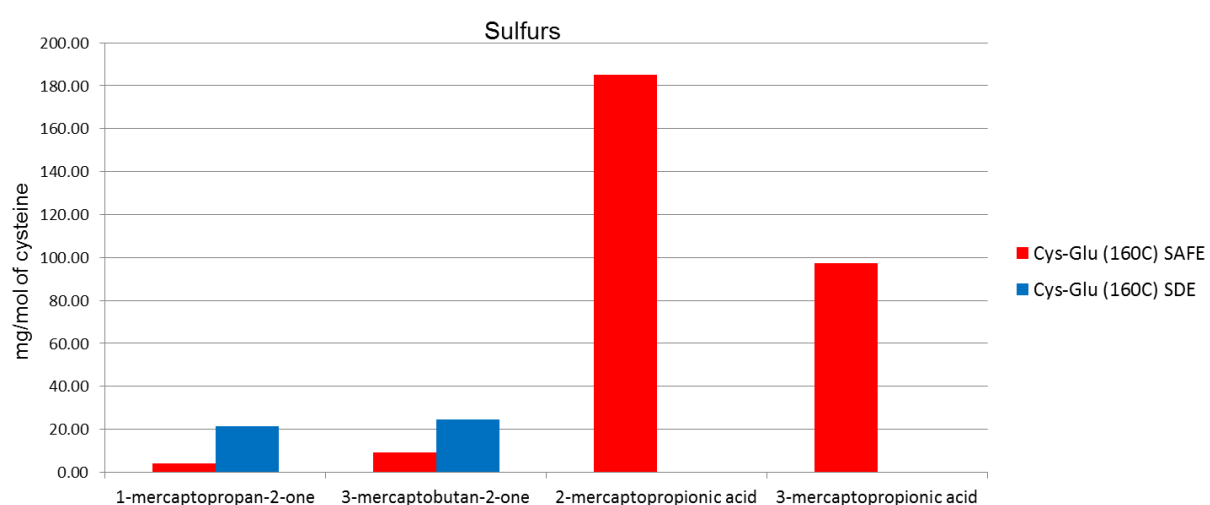
Table 4.4 A comparison of high impact, low concentration sulfur compounds in both the SDE and SAFE extracts.



Additional data comparing volatile sulfur chemistry between SAFE and SDE is shown in Table 4.5. Both 1-mercaptoopropan-2-one and 3-mercaptobutan-2-one are high impact sulfur compounds found at even higher levels than the sulfur compounds reported in Table 4.4. There are also significant concentration differences for these compounds between SAFE and SDE which trends similarly to the increased values from the thermal processing of SDE. However, the biggest surprise and opposite trend was observed when comparing the concentration of 2-mercapto propionic acid (2MPA; CAS 79-42-5) and 3-mercapto propionic acid (3MPA; CAS 107-96-0) in both the SAFE

and SDE extracts. As shown in Figure 4.7, both 2MPA and 3MPA were measured as the two highest concentration compounds in the SAFE extract but neither were detected by SDE.

Table 4.5 A comparison of high impact, high concentration sulfur compounds in both the SDE and SAFE extracts.



Like the Strecker acids discussed by Hofmann et al. (Hofmann, Munch & Schieberle, 2000), both 2MPA and 3MPA are formed from the intact skeleton of cysteine and will be furthered discussed in the next section. The fact that SDE does not detect both 2MPA and 3MPA, which are the largest concentration volatile compounds in the SAFE extract, is a major shortcoming. Similar findings were recorded by Zhang & Ho from the reaction of Cys-Glu using SDE (Zhang & Ho, 1991), as well as by Umamo et al. who used glass tube traps to collect the volatiles generated in the headspace during the reaction (Umamo, Hagi, Nakahara, Shyoji & Shibamoto, 1995). Both sets of research did not detect 2MPA and 3MPA. A hypothesis for this outcome deals with the

hydrophilicity of both compounds. If 2MPA and 3MPA are less likely to be liberated in the vapor phase, it would limit the extraction efficiency of each compound by SDE. Liquid-liquid extraction followed by SAFE is more successful at not only limiting thermal artifact formation, but shows little discrimination for polar, hydrophilic, less volatile, and unstable constituents. To prove out this hypothesis, additional analysis of the physico-chemical properties of 2MPA and 3MPA was completed in the following sections.

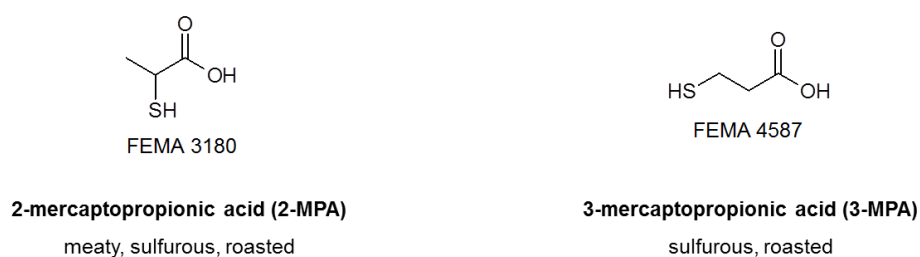


Figure 4.7 The structures and odor descriptors of 2MPA and 3MPA from the Cys-Glu reaction.

4.2.2 Formation of Mercapto Acids

Few references in the literature discuss 2MPA and 3MPA in Maillard reactions. Tai & Ho identified 3MPA in the reaction of glutathione and glucose at pH 3.0 (Tai & Ho, 1998), while Hofmann & Schieberle identified both 2MPA and 3MPA in the reaction of cysteine and ribose at pH 5.0 (Hofmann & Schieberle, 1995). In 1994, Tressl et al. studied the formation of both 2MPA and 3MPA through carbon labeling of cysteine in the thermal reaction with glucose (Tressl, Kersten, Nittka & Rewicki, 1994). Both

Figure 4.8 and Figure 4.9 show the initial condensation of cysteine and glucose to form a Schiff base. In Figure 4.8, Strecker degradation is led by the transamination of 2-oxo-3-mercaptopropionic acid and reduction of this alpha-keto acid to form 3MPA. In Figure 4.9, Strecker degradation is instead dominated by beta-elimination of hydrogen sulfide and the formation of pyruvate, followed by the addition of hydrogen sulfide to form 2MPA. Based on the carbon labeling, Tressl et al. concluded that both 2MPA and 3MPA formed from the intact carbon skeleton of cysteine.

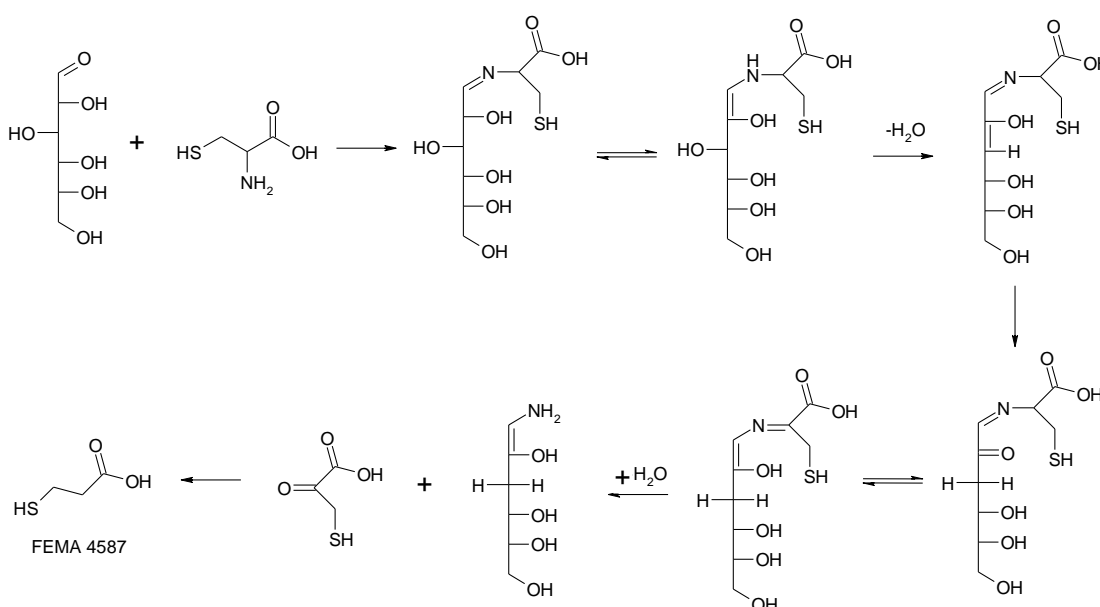


Figure 4.8 The formation of 3MPA by transamination of 2-oxo-3-mercaptopyruvate and reduction of alpha-keto acid (adapted from Tressl, Kersten, Nittka & Rewicki, 1994).

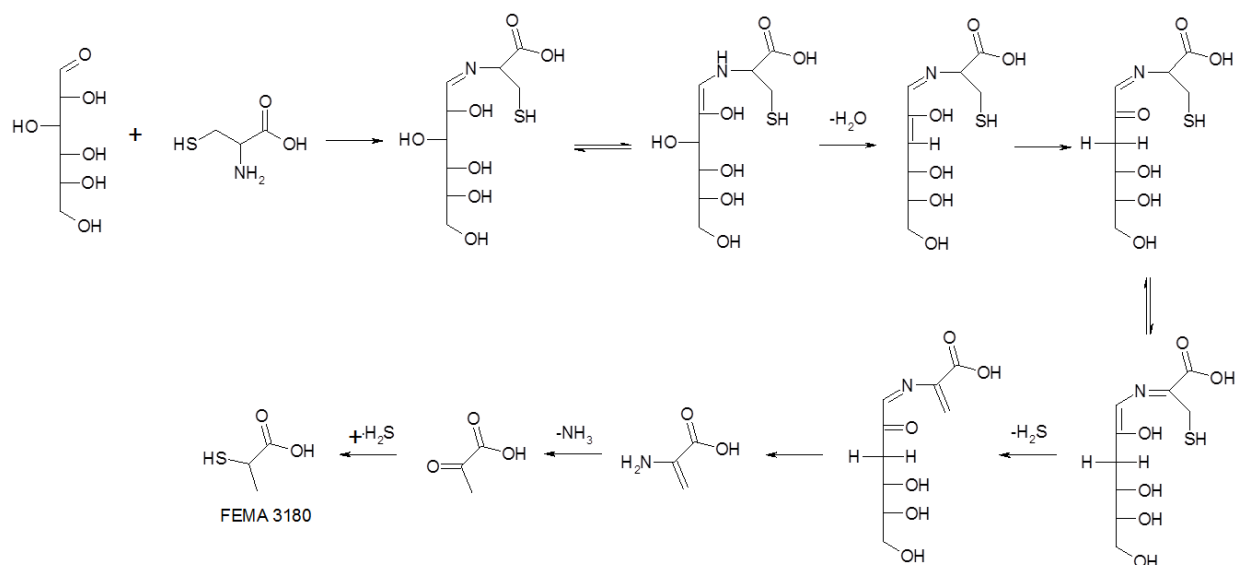


Figure 4.9 The formation of 2MPA by beta-elimination of hydrogen sulfide (adapted from Tressl, Kersten, Nittka & Rewicki, 1994).

From a similar model system of Cys-Glu, 2MPA and 3MPA measured low odor activity values in an AEDA study by Hofmann & Schieberle (Hofmann & Schieberle, 1997). However, both mercapto acids were not detected as key odorants in the cysteine-rhamnose model system under similar reaction conditions, thereby suggesting these compounds are preferentially generated from the reaction with glucose rather than rhamnose.

4.2.3 Physico-Chemical Properties of Mercapto Acids

To study the hydrophobicity of 2MPA and 3MPA, an experiment was designed to determine the $\log_{10}P_{ow}$ by HPLC. Like the standard materials, both 2MPA and 3MPA are retained on the C8 column in proportion to their hydrocarbon-water partition

coefficient. Water-soluble compounds elute first, followed by oil-soluble compounds. The relationship between the retention time on a C8 column and hydrophobicity can be established. The partition coefficient is calculated from the capacity factor k , given by the expression $k = (t_r - t_0) / t_0$ where, t_r is the retention time of the test substance, and t_0 is the dead-time or the average time a solvent molecule needs to pass the column. The results of the standard materials, 2MPA, and 3MPA are shown in Table 4.6. The $\log_{10}P_{ow}$ of 3MPA was determined to be 0.3 +/- 0.1 at 25°C, while the $\log_{10}P_{ow}$ of 2MPA was determined to be 0.6 +/- 0.1 at 25°C.

Table 4.6 The measured $\log_{10}P_{ow}$ values for duplicate measurements of 2MPA and 3MPA.

Sample	Component	t_r (min.)	k	$\log_{10}k$	$\log_{10}P_{ow}$
t_0	formamide	1.49			
Standard Run A	benzyl alcohol	1.94	0.300	-0.523	1.1
	cinnamic alcohol	2.22	0.491	-0.309	1.9
	allyl phenyl ether	3.68	1.470	0.167	2.9
	benzyl benzoate	5.09	2.417	0.383	4.0
	n-butyl benzene	9.88	5.629	0.750	4.6
	4,4"-DDT	25.98	16.438	1.216	6.2
Sample A	3-mercaptopropionic acid (3MPA)	1.72	0.153	-0.815	0.3
Sample B	3-mercaptopropionic acid (3MPA)	1.72	0.152	-0.817	0.3
Sample A	2-mercaptopropionic acid (2MPA)	1.79	0.199	-0.700	0.6
Sample B	2-mercaptopropionic acid (2MPA)	1.79	0.199	-0.700	0.6
Standard Run B	benzyl alcohol	1.94	0.301	-0.522	1.1
	cinnamic alcohol	2.22	0.492	-0.308	1.9
	allyl phenyl ether	3.69	1.473	0.168	2.9
	benzyl benzoate	5.10	2.423	0.384	4.0
	n-butyl benzene	9.90	5.647	0.752	4.6
	4,4"-DDT	26.11	16.523	1.218	6.2

*4,4"-DDT: 4,4'-dichlorodiphenyltrichloroethane

These measured values are some of the lowest recorded using this method. In comparison, butyric acid and hexanoic acid, which both have similar chemistry to 2MPA and 3MPA, measured $\log_{10}P_{ow}$ of 0.8 and 1.9 respectively (Sangster, 1989). This data demonstrates the hydrophilicity of both 2MPA and 3MPA. SDE will ineffectively liberate these molecules from the water phase into the vapor phase to be condensed and extracted with diethyl ether.

4.3 Maillard Reaction of Arginine/Cysteine-Glucose

The initial data from the single amino acid (arginine or cysteine) with glucose was established in the previous sections. The final measurements in this study focus on the identification of the volatiles formed from the reaction of two amino acids (arginine and cysteine) with glucose. Knowing how each individual amino acid reacts with glucose will help to determine the preferential and competitive reactions that take place when two amino acids are reacted together.

In this reaction, both arginine and cysteine were added at equal molar concentrations and reacted with glucose. Like the Arg-Glu reaction, the analytical and sensory data for three different reaction temperatures (100 °C, 130 °C, 160 °C) were acquired at an adjusted pH of 7.4 (initial pH 5.9). There were clear differences in the color at the three different reaction temperatures as shown in Figure 4.10. At 100 °C, there was a slight eggy aroma with no color change observed. Only a couple trace compounds were identified at this reaction temperature. At 130 °C, a medium intensity roasted, meaty aroma was observed with a light-yellow color. This temperature yielded low

concentrations of furans and sulfurs. Finally, at 160 °C, the pH had dropped to 4.2 by the end of the reaction and a stronger roasted, meat aroma was detected along with a deeper orange color. The chromatogram for this reaction yielded a series of furans/pyrans and sulfur compounds.



Figure 4.10 Three reactions of Arg/Cys-Glu. From left to right: Arg/Cys-Glu at 100 °C at pH 7.4; Arg/Cys-Glu at 130 °C at pH 7.4; Arg/Cys-Glu at 160 °C at pH 7.4.

The analytical data for these reactions can be found in Table 4.7. The total concentration of volatile compounds clearly increases as the temperature of the reaction increases. There were unfavorable conditions for pyrazine formation, which could be due to several reasons. As shown in the Arg-Glu reaction, pyrazine formation is favored by more basic conditions (pH 10.4 instead of pH 7.4), whereby increased sugar fragmentation yields secondary intermediates (glyoxal and methyl glyoxal) that readily react with free ammonia or the amino group of arginine. Secondly, it appears that the thiol group of cysteine inhibits sugar fragmentation and blocks arginine interaction in the formation of pyrazines as discussed in previous sections. Schubert showed that the thiol group of cysteine is highly reactive with glyoxals (Schubert, 1935), like

methylglyoxal and phenylglyoxal, although not as reactive as arginine (Takahashi, 1977).

Table 4.7 The analytical data from the Arg/Cys-Glu reactions.

Compound	OV1 (Kovats)	Arg- Cys-Glu (100 °C) SAFE pH 7.4*	Arg- Cys-Glu (130 °C) SAFE pH 7.4*	Arg- Cys-Glu (160 °C) SAFE pH 7.4*
pyrazines				
pyrazine	716	0.02	0.02	0.06
2-methylpyrazine	804	nd	nd	0.47
2,6- + 2,5-dimethylpyrazine	891	nd	nd	nd
2-ethylpyrazine	898	nd	nd	nd
2,3-dimethylpyrazine	898	nd	nd	nd
2-vinylpyrazine	928	nd	nd	nd
2-ethyl-6-methylpyrazine	978	nd	nd	nd
2-ethyl-5-methylpyrazine	981	nd	nd	nd
2,3,5-trimethylpyrazine	988	nd	nd	nd
2-methyl-5-vinylpyrazine	998	nd	nd	nd
quinoxaline	1173	nd	nd	nd
<i>total pyrazines</i>		0.02	0.02	0.52
furans/pyrans				
furfural	809	nd	nd	nd
furfuryl alcohol	828	nd	nd	5.11
2-acetylfuran	890	nd	nd	1.85
5-methylfurfural	939	nd	nd	1.70
5-methyl-2-furanmethanol	947	nd	nd	0.48
furaneol	1030	nd	0.13	1.36
5-hydroxy-5,6-dihydromaltol	1116	nd	1.15	3.52
5-hydroxymethylfurfural	1177	nd	nd	nd
<i>total furans/pyrans</i>		0.00	1.28	14.03
thiophenes				
thiophene	647	nd	nd	0.67
2-methylthiophene	757	nd	nd	0.38
2,5-dimethylthiophene	861	nd	nd	nd
2-ethylthiophene	852	nd	nd	0.81
2-formylthiophene	975	nd	nd	2.51
2-acetylthiophene	1074	nd	nd	2.01
2-formyl-4-methylthiophene	1091	nd	nd	4.51
tetrahydrothiophen-3-one	920	nd	nd	3.22
3-thiophenethiol	950	nd	nd	3.98
2-methyltetrahydrothiophen-3-one	958	nd	nd	1.86
3-mercapto-2-methylthiophene	1054	nd	nd	1.74

2,5-dimethyl-4-hydroxy-3(2h)-thiophenone	1134	nd	nd	13.57
thieno[3.2.b]thiophene	1176	nd	nd	1.56
2,5-dimethyl-2,4-dihydroxy-3(2h)-thiophenone	1223	0.00	0.00	36.82
<i>total thiophenes</i>		nd	0.00	73.64
misc. sulfurs				
methyl mercaptan	484	nd	nd	nd
1,1-ethanedithiol	715	nd	nd	nd
2-mercaptoethanol	769	nd	nd	nd
1-mercaptopropan-2-one	749	nd	0.15	3.40
3-mercaptopentan-2-one	791	nd	0.14	4.99
1,2-ethanedithiol	801	nd	nd	nd
1-mercaptopentan-3-one	850	nd	nd	nd
1-mercaptopentan-2-one	852	nd	nd	nd
2-methylfuran-3-thiol	853	nd	nd	nd
3-mercaptopentan-2-one	881	nd	nd	nd
2-mercaptopentan-3-one	886	nd	nd	nd
furfuryl mercaptan	895	nd	nd	0.30
2-(1-mercaptoethyl)-furan	932	nd	nd	nd
5-methyl-2-furanmethanethiol	994	nd	nd	nd
2-mercaptopropionic acid	985	nd	nd	216.46
3-mercaptopropionic acid	998	nd	nd	42.39
3,5-dimethyl-1,2,4-trithiolane isomer i	1112	nd	nd	nd
3,5-dimethyl-1,2,4-trithiolane isomer ii	1119	nd	nd	nd
1,2-dithian-4-one	1124	nd	nd	nd
5-acetyl-2,3-dihydro-1,4-thiazine	1322	nd	0.07	nd
<i>total misc sulfurs</i>		0.00	0.36	267.53
misc.				
1-hydroxypropan-2-one	622	nd	nd	nd
acetoin	680	nd	nd	0.32
cyclopentanone	763	nd	nd	nd
cyclohexan-1,2-dione	974	nd	nd	nd
cyclotene	997	nd	nd	nd
2-aminophenol	1177	nd	nd	nd
benzene-1,2-diol	1168	nd	nd	nd
acetaldehyde	485	0.18	0.16	0.20

nd – not detected; * Data reported in mg/mol of arginine from the average of two runs.

Both DMHT and DMDHT increased significantly in the Arg/Cys-Glu reaction compared to the Cys-Glu reaction. This was a surprising result and seems to suggest that the addition of arginine helps to increase the degradation of glucose and release of

hydrogen sulfide from cysteine, as both are requirements for DMHT and DMDHT generation. Like the Cys-Glu reaction, 5HMF was not detected in the Arg/Cys-Glu model system. The thiol group appears to competitively bind with amines and block certain secondary intermediates that would generate 5HMF, as also shown by Haleva-Toledo et al. (Haleva-Toledo, Naim, Zehavi & Rouseff, 1999).

As Table 4.7 shows, several compounds (either nitrogen or sulfur containing) were detected in both the Cys-Glu and Arg/Cys-Glu model systems, including pyrazines and thiophenes. However, only a few low level thiazoles, thiazines, and thiazolidines (nitrogen and sulfur containing compounds) were detected (data not shown). This goes against the typical understanding of these sorts of reactions, where both alkyl and acyl compounds are typically detected (Umano, Hagi, Nakahara, Shyoji & Shibamoto 1995). In fact, the data generated by Umano et al. found that at pH 8, there is optimal conditions for thiazolidine formation. In addition, very few pyridines, pyrroles and oxazoles were detected in all three reactions, which is not surprising as these amino acids may not generate the precursors for these types of products as readily as other amino acids (Hwang, Hartman & Ho, 1995).

Conclusions

The goal of this research was to increase our understanding of the Maillard reaction by measuring the volatile compounds formed from the addition of one or two amino acids with glucose. Data has shown that temperature, pH, and extraction technique can influence the final concentration of odorants. The Strecker aldehyde of arginine was most likely not identified due to the extraction procedure and instrumental design. Additional acid/base extraction and HPLC may increase the chances for identification. Instead, the comparison of extraction by SAFE and SDE for the Cys-Glu reaction was informative, most notably for the recovery and quantitation of high impact sulfurs, including mercapto acids like 2MPA and 3MPA.

5.1 Future Work

Next steps in this study will include the addition of a third and fourth amino acid to the reaction to continue to understand the volatiles that are formed from these competitive interactions. Additional work will also include the addition of phenolic compounds to these same reactions to study the effect of carbonyl trapping on the volatile profiles of Maillard reactions. This phenomenon has been explored over the last decade in the literature, mainly incorporating simple model systems where carbonyl compounds are reacted with single polyphenols as shown Figure 5.1 (Totlani & Peterson, 2006; Zamora, Aguilar & Hidalgo, 2017; Hidalgo, Aguilar & Zamora, 2017). There have also been a few references where polyphenols were added to simple Maillard model systems (Noda & Peterson, 2007; Kokkinidou & Peterson, 2014; Troise, Fiore, Colantuono,

Kokkinidou, Peterson & Fogliano, 2014; Jansson, Rauh, Danielsen, Poojary, Waehrens, Bredie, Sorensen, Petersen, Ray & Lund, 2017).

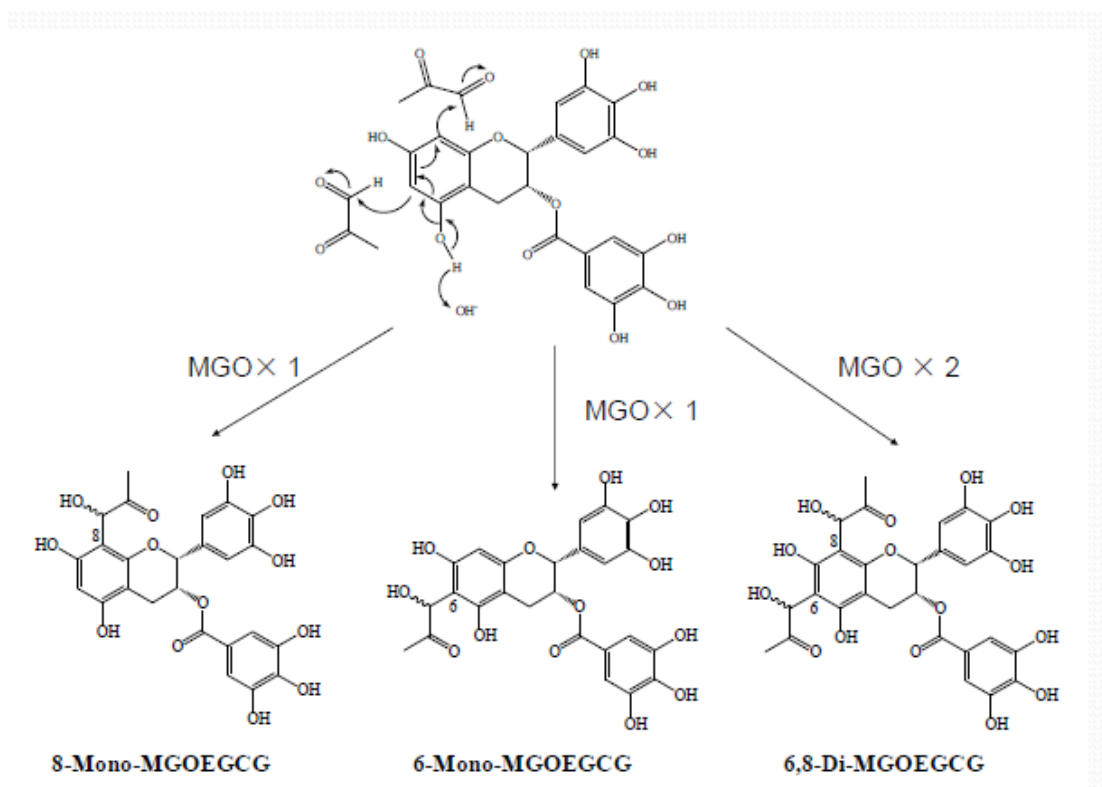


Figure 5.1 Examples of epigallocatechin-3-gallate (EGCG) reacting with one or two equivalents of methylglyoxal (MGO) in both the 6- and 8-position of the polyphenol (adapted from Wang & Ho, 2012).

More recently, research has moved to study the addition of polyphenols in more complex matrices, including Maillard reactions. This is where additional research is required to understand how certain reactive intermediates, like glyoxal and methylglyoxal, are deactivated by the irreversible binding to polyphenols. Research will focus on common, individual polyphenols like quercetin and catechin. Finally, the

addition of natural herbs and spices like tea and cinnamon, which are known to have high levels of polyphenols, will be compared to individual polyphenols to determine the effectiveness of carbonyl trapping during the Maillard reaction.

References

- Acree, T. E.; Barnard, J.; Cunningham, D. G. A procedure for the sensory analysis of gas chromatographic effluents. *Food Chem.* **1984**, *14*, 273-286.
- Adams, A.; Polizzi, V.; van Boekel, M.; De Kimpe, N. Formation of pyrazines and a novel pyrrole in Maillard model systems of 1,3-dihydroxyacetone and 2-oxopropanal. *J. Agric. Food Chem.* **2008**, *56*, 2147-2153.
- Bemelmans, J. M. H. Review of isolation and concentration techniques. In: Land, G. G.; Nursten, H. E., editors. *Progress in Flavour Research*. London: Applied Sciences; 1979, p. 79–88.
- Bohnenstengel, C.; Baltes, W. Model reactions on roast aroma formation. XII. Reaction of glucose with aspartic acid or asparagine at three different temperatures. *Z. Lebensm. Unters. Forsch.* **1992**, *194*, 366-371.
- Brands, C. M. J.; van Boekel, M. A. J. S. Reactions of monosaccharides during heating of sugar-casein systems: building of a reaction network model. *J. Agric. Food Chem.* **2001**, *49*, 4667-4675.
- Cerny, C.; Davidek, T. Formation of aroma compounds from ribose and cysteine during the Maillard reaction. *J. Agric. Food Chem.* **2003**, *51*, 2714-2721.
- Chaintreau, A. Simultaneous distillation-extraction: from birth to maturity-review. *Flav. Frag. J.* **2001**, *16*, 136-148.
- Creighton, T. E. Chemical properties of polypeptides. In *Proteins: Structures and Molecular Principles*; Freeman: New York, 1984; pp 10-13.

- de Roos, K. B.; Wolswinkel, K.; Sipma, G. Amadori compounds of cysteine and their role in the development of meat flavor. In *Process and Reaction Flavors*; ACS Symposium Series; American Chemical Society: Washington, DC 2005; pp 117-129.
- Engel, W.; Bahr, W.; Schieberle, P. Solvent assisted flavour evaporation – a new and versatile technique for the careful and direct isolation of aroma compounds from complex food matrices. *Eur. Food. Res. Technol.* **1999**, *209*, 237-241.
- Farkas, P.; Sadecka, J.; Kovac, M.; Siegmund, B.; Leitner, E.; Pfannhauser, W. Key odorants of pressure-cooked hen meat. *Food Chem.* **1997**, *60*, 617-621.
- Friedman, M.; Molnar-Perl, I. Inhibition of browning by sulfur amino acids. 1. Heat amino acid-glucose systems. *J. Agric. Food Chem.* **1990**, *38*, 1642-1647.
- Gasser, U.; Grosch, W. Primary odorants of chicken broth. A comparative study with meat broths from cow and ox. *Z. Lebensm. Unters. Forsch.* **1990**, *190*, 3-8.
- Glomb, M. A.; Lang, G. Isolation and characterization of glyoxal-arginine modifications. *J. Agric. Food Chem.* **2001**, *49*, 1493-1501.
- Gökmen, V.; Açar, O, C.; Koksel, H.; Acar, J. Effects of dough formula and baking conditions on acrylamide and hydroxymethylfurfural formation in cookies. *Food Chem.* **2007**, *104*, 1136-1142.
- Haberhauer-Troyer, C.; Rosenberg, E.; Grasserbauer, M. Evaluation of solid-phase microextraction for sampling of volatile organic sulfur compounds in air for subsequent gas chromatographic analysis with atomic emission detection. *J. Chrom. A.* **1999**, *848*, 305-315.

- Haffenden, L. J. W.; Yaylayan, V. A. Mechanism of formation of redox-active hydroxylated benzenes and pyrazine in ^{13}C -labeled glycine/d-glucose model systems. *J. Agric. Food Chem.* **2005**, *53*, 9742-9746.
- Haleva-Toledo, E.; Naim, M.; Zehavi, U.; Rouseff, R. L. Effects of L-cysteine and N-acetyl-L-cysteine on 4-hydroxy-2,5-dimethyl-3(2h)-furanone (furanol), 5-(hydroxymethyl)furfural, and 5-methylfurfural formation and browning in buffer solutions containing either rhamnose or glucose and arginine. *J. Agric. Food Chem.* **1999**, *47*, 4140-4145.
- Hayase, F.; Konishi, Y.; Kato, H. Identification of the modified structure of arginine residues in proteins with 3-deoxyglucosone, a Maillard reaction intermediate. *Biosci, Biotech. Biochem.* **1995**, *59*, 1407-1411.
- Hidalgo, F. J.; Aguilar, I.; Zamora, R. Model studies on the effect of aldehyde structure on their selective trapping by phenolic compounds. *J. Agric. Food Chem.* **2017**, *65*, 4736-4743.
- Hodge, J. E. Chemistry of browning reactions in model systems. *J. Agric. Food Chem.* **1953**, *1*, 928-943.
- Hofmann, T.; Schieberle, P. Evaluation of the key odorants in a thermally treated solution of ribose and cysteine by aroma extract dilution techniques. *J. Agric. Food Chem.* **1995**, *43*, 2187-2194.
- Hofmann, T.; Schieberle, P. Identification of potent aroma compounds in thermally treated mixtures of glucose/cysteine and rhamnose/cysteine using aroma extract dilution techniques. *J. Agric. Food Chem.* **1997**, *45*, 898-906.

- Hofmann, T.; Schieberle, P. Identification of key aroma compounds generated from cysteine and carbohydrates under roasting conditions. *Z. Lebensm. Unters. Forsch. A.* **1998**, *207*, 229-236.
- Hofmann, T.; Munch, P.; Schieberle, P. Quantitative model studies on the formation of aroma-active aldehydes and acids by Strecker-type reactions. *J. Agric. Food Chem.* **2000**, *48*, 434-440.
- Hou, L.; Xie, J.; Zhao, J.; Zhao, M.; Fan, M.; Xiao, Q.; Liang, J.; Chen, F. Roles of different initial Maillard intermediates and pathways in meat flavor formation for cysteine-xylose-glycine model reaction systems. *Food Chem.* **2017**, *232*, 135-144.
- Huang, T.-C.; Bruechert, L. J.; Ho, C.-H. Kinetics of pyrazine formation in amino acid-glucose systems. *J. Food Sci.* **1989**, *54*, 1611-1614.
- Hwang, H.-I.; Hartman, T. G.; Rosen, R. T.; Lech, J.; Ho, C.-T. Formation of pyrazines from the Maillard reaction of glucose and lysine- α -amine- ^{15}N . *J. Agric. Food Chem.* **1994**, *42*, 1000-1004.
- Hwang, H.-I.; Hartman, T. G.; Ho, C.-T. Relative reactivities of amino acids in pyrazine formation. *J. Agric. Food Chem.* **1995**, *43*, 179-184.
- Hwang, H.-I.; Hartman, T. G.; Ho, C.-T. Relative reactivities of amino acids in the formation of pyridines, pyrroles, and oxazoles. *J. Agric. Food Chem.* **1995**, *43*, 2917-2921. (B)
- Hwang, I. G.; Woo, K. S.; Kim, D. J.; Hong, J. T.; Hwang, B. Y.; Lee, Y. R.; Jeong, H. S. Isolation and identification of an antioxidant substance from heated garlic (*Allium sativum* L.). *Food Sci. Biotech.* **2007**, *16*, 963-966.

- Jansson, T.; Rauh, V.; Danielsen, B. P.; Poojary, M. M.; Waehrens, S. S.; Bredie, W. L. P.; Sorensen, J.; Petersen, M. A.; Ray, C. A.; Lund, M. N. Green tea polyphenols decrease Strecker aldehydes and bind to proteins in lactose-hydrolyzed UHT milk. *J. Agric. Food Chem.* **2017**, *65*, 10550-10561.
- Kato, S.; Kurata, T.; Fujimaki, M. Volatile compounds produced by the reaction of l-cysteine or l-cystine with carbonyl compounds. *Agr. Biol. Chem.* **1973**, *37*, 539-544.
- Kersch, R.; Grosch, W. Quantification of 2-methyl-3-furanthiol, 2-furfurylthiol, 3-mercapto-2-pentanone, and 2-mercapto-3-pentanone in heated meat. *J. Agric. Food Chem.* **1998**, *46*, 1954-1958.
- Klopfer, A.; Spanneberg, R.; Glomb, M. A. Formation of arginine modifications in a model system of N^α-tert-butoxycarbonyl (Boc)-arginine with methylglyoxal. *J. Agric. Food Chem.* **2011**, *59*, 394-401.
- Kobayasi, N.; Fujimaki, M. On the formation of mercaptoacetaldehyde, hydrogen sulfide and acetaldehyde on boiling cysteine with carbonyl compounds. *Agr. Biol. Chem.* **1965**, *29*, 698-699.
- Kokkinidou, S.; Peterson, D. G. Control of Maillard-type off-flavor development in ultrahigh-temperature-processed bovine milk by phenolic chemistry. *J. Agric. Food Chem.* **2014**, *62*, 8023-8033.
- Lee, H. S.; Nagy, S. Relative reactivities of sugars in the formation of 5-hydroxymethylfurfural in sugar-catalyst model systems. *J. Food Proc. Preserv.* **1990**, *14*, 171-178.

- Likens, S. T.; Nickerson, G. B. Detection of certain hop oil constituents in brewing products. *Proc. Am. Soc. Brewing Chem.* **1964**, 5-13.
- Lund, M. N.; Ray, C. A. Control of Maillard reactions in foods: strategies and chemical mechanisms. *J. Agric. Food Chem.* **2017**, *65*, 4537-4552.
- Molina-Calle, M.; Sanchez de Medina, V.; Priego-Capote, F.; Luque de Castro, M. D. Establishing compositional differences between fresh and black garlic by a metabolomics approach based on LC-QTOF MS/MS analysis. *J. Food Comp. Anal.* **2017**, *62*, 155-163.
- Mottram, D. S.; Nobrega, I. C. C. Formation of sulfur aroma compounds in reaction mixtures containing cysteine and three different forms of ribose. *J. Agric. Food Chem.* **2002**, *50*, 4080-4086.
- Mottram, D. S.; Elmore, J. S. Control of the Maillard reaction during the cooking of food. In *Controlling Maillard Pathways to Generate Flavors*; ACS Symposium Series; American Chemical Society: Washington, DC 2010; pp 143-155.
- Mulders, E. J. Volatile components from the non-enzymic browning reaction of the cysteine/cysteine-ribose system. *Z. Lebensm Unters. –Forsch.* **1973**, *152*, 193-201.
- Munch, P.; Hofmann, T.; Schieberle, P. Comparison of key odorants generated by thermal treatment of commercial and self-prepared yeast extracts: influence of the amino acid composition on odorant formation. *J. Agric. Food Chem.* **1997**, *45*, 1338-1344.

- Noda, Y.; Peterson, D. G. Structure-reactivity relationships of flavan-3-ols on product generation in aqueous glucose/glycine model systems. *J. Agric. Food Chem.* **2007**, *55*, 3686-3691.
- Nursten, H. The chemistry of nonenzymic browning. In *The Maillard Reaction: Chemistry, Biochemistry and Implications*; The Royal Society of Chemistry: Cambridge, UK 2005; pp 6-30.
- Pathy, L.; Smith, E. L. Reversible modification of arginine residues. Application to sequence studies by restriction of tryptic hydrolysis to lysine residues. *J. Bio. Chem.* **1975**, *250*, 557-564.
- Pelusio, F.; Nilsson, T.; Montanarella, L.; Tilio, R.; Larsen, B.; Facchetti, S.; Mødsen, J. O. Headspace solid-phase microextraction analysis of volatile organic sulfur compounds in black and white truffle aroma. *J. Agric. Food Chem.* **1995**, *43*, 2138-2143.
- Piloty, M.; Baltes, W. Investigations on the reaction of amino-acids with α -dicarbonyl compounds. I. Reactivity of amino-acids in the reaction with α -dicarbonyl compounds. *Z. Lebensm. Unters. Forsch. A.* **1979**, *168*, 368-373.
- Rouseff, R. L. Analytical methods to determine volatile sulfur compounds in foods and beverages. In *Heteroatomic Aroma Compounds*; ACS Symposium Series; American Chemical Society: Washington, DC 2002; pp 2-24.
- Samsudin, M. W.; Rongtao, S.; Said, I. M. Volatile compounds produced by the reaction of leucine and valine with glucose in propylene glycol. *J. Agric. Food Chem.* **1996**, *44*, 247-250.

- Sandra, P.; Baltussen, E.; David, F.; Cramers, C. Stir bar sorptive extraction (SBSE), a novel extraction technique for aqueous samples: theory and principles. *J. Microcolumn Separations*. **1999**, *11*, 737-747.
- Sangster, J. Octanol-water partition coefficients of simple organic compounds. *J. Phys. Chem Ref. Data*. **1989**, *18*, 1111-1227.
- Satoh, M.; Nomi, Y.; Yamada, S.; Takenaka, M.; Ono, H.; Murata, M. Identification of 2,4-dihydroxy-2,5-dimethyl-3(2H)-thiophenone as a low-molecular-weight yellow pigment in soy sauce. *Biosci. Biotech. Biochem.* **2011**, *75*, 1240-1244.
- Schieberle, P.; Grosch, W. Evaluation of the flavor of wheat and rye bread crusts by aroma extract dilution analysis. *Z. Lebensm. Unters. Forsch.* **1987**, *185*, 111-113.
- Schieberle, P.; Grosch, W. Quantitative analysis of aroma compounds in wheat and rye bread crusts using a stable isotope dilution assay. *J. Agric. Food Chem.* **1987**, *35*, 252-257. (B)
- Schubert, M. P. Combination of thiol acids with methylglyoxal. *J. Bio. Chem.* **1935**, *III*, 671-678.
- Schwarzenbolz, U.; Henle, T.; Haefner, R.; Klostermeyer, H. On the reaction of glyoxal with proteins. *Z. Lebensm. Unters. Forsch. A.* **1997**, *205*, 121-124.
- Shibamoto; T.; Yeo, H. Flavor in the cysteine-glucose model system prepared in microwave and conventional ovens. In *Thermally Generated Flavors*; ACS Symposium Series; American Chemical Society: Washington, DC 1993; pp 457-465.

- Shu, C.-K.; Hagedorn, M. L.; Mookherjee B. D.; Ho, C.-T. Two novel 2-hydroxy-3(2H)-thiophenones from the reaction between cystine and 2,5-dimethyl-4-hydroxy-3(2H)-furanone. *J. Agric. Food Chem.* **1985**, *33*, 638-641.
- Shu, C.-K.; Hagedorn, M. L.; Mookherjee, B. D.; Ho, C. -T. pH effect on the volatile components in the thermal degradation of cysteine. *J. Agric. Food Chem.* **1985**, *33*, 442-446. (b)
- Shu, C.-K.; Hagedorn, M. L.; Ho, C.-T. Two novel thiophenes from the reaction of cysteine and 2,5-dimethyl-4-hydroxy-3(2H)-furanone. *J. Agric. Food Chem.* **1986**, *34*, 344-346.
- Shu, C.-K.; Ho, C.-T. Effect of pH on the volatile formation from the reaction between cysteine and 2,5-dimethyl-4-hydroxy-3(2H)-furanone. *J. Agric. Food Chem.* **1988**, *36*, 801-803.
- Shu, C.-K. Degradation products formed from glucosamine in water. *J. Agric. Food Chem.* **1998**, *46*, 1129-1131.
- Shu, C.-K. Flavor compounds generated from inulin. *J. Agric. Food Chem.* **1998**, *46*, 1964-1965. (b)
- Sohn, M.; Ho, C. -T. Ammonia generation during thermal degradation of amino acids. *J. Agric. Food Chem.* **1995**, *43*, 3001-3003.
- Sweeley, C. C.; Elliott, W. H.; Fries, I.; Ryhage, R. Mass spectrometric determination of unresolved components in gas chromatographic effluents. *Anal. Chem.* **1966**, *38*, 1549-1553.

- Tai, C.-Y.; Ho, C. -T. Influence of glutathione oxidation and pH on thermal formation of Maillard-type volatile compounds. *J. Agric. Food Chem.* **1998**, *46*, 2260-2265.
- Takahashi, K. The reaction of phenylglyoxal with arginine residues in proteins. *J. Bio. Chem.* **1968**, *243*, 6171-6179.
- Takahashi, K. The reactions of phenylglyoxal and related reagents with amino acids. *J. Biochem.* **1977**, *81*, 395-402.
- Toi, K.; Bynum, E.; Norris, E.; Itano, H. A. Studies on the chemical modification of arginine. I. The reaction of 1,2-cyclohexanedione with arginine and arginyl residues of proteins. *J. Bio. Chem.* **1967**, *242*, 1036-1043.
- Totlani, V. M.; Peterson, D. G. Epicatechin carbonyl-trapping reactions in aqueous Maillard systems: identification and structural elucidation. *J. Agric. Food Chem.* **2006**, *54*, 7311-7318.
- Tressl, R.; Helak, B.; Martin, N.; Kersten, E. Formation of amino acid specific Maillard products and their contribution to thermally generated aromas. In *Thermal Generation of Aromas; ACS Symposium Series; American Chemical Society: Washington, DC 1989; pp 156-171.*
- Tressl, R.; Kersten, E.; Nittka, C.; Rewicki, D. Formation of sulfur-containing flavor compounds from [13C]-labeled sugars, cysteine, and methionine. In *Sulfur Compounds in Foods; ACS Symposium Series; American Chemical Society: Washington, DC 1994; pp 224-235.*
- Troise, A. D.; Fiore, A.; Colantuono, A.; Kokkinidou, S.; Peterson, D. G.; Fogliano, V. Effect of olive mill wastewater phenol compounds on reactive carbonyl species

- and Maillard reaction end-products in ultrahigh-temperature-treated milk. *J. Agric. Food Chem.* **2014**, *62*, 10092-10100.
- Umamo, K.; Hagi, Y.; Nakahara, K.; Shyoji, A.; Shibamoto, T. Volatile chemicals formed in the headspace of a heated D-glucose/L-cysteine Maillard model system. *J. Agric. Food Chem.* **1995**, *43*, 2212-2218.
- Van den Dool, H.; Kratz, P. D. A generalization of the retention index system including linear temperature programmed gas-liquid partition chromatography. *J. Chrom.* **1963**, *11*, 463-471.
- Vas, G.; Vekey, K. Solid-phase microextraction: a powerful sample preparation tool prior to mass spectrometric analysis. *J. Mass Spec.* **2004**, *39*, 233-254.
- Wang, Y.; Ho, C.-T. Formation of 2,5-dimethyl-4-hydroxy-3(2H)-furanone through methylglyoxal: a Maillard reaction intermediate. *J. Agric. Food Chem.* **2008**, *56*, 7405-7409.
- Wang, Y.; Ho, C.-T. Flavour chemistry of methylglyoxal and glyoxal. *Chem. Soc. Rev.* **2012**, *41*, 4140-4149.
- Wang, Y.; Juliani, H. R.; Simon, J. E.; Ho, C.-T. Amino acid-dependent formation pathways of 2-acetylfuran and 2,5-dimethyl-4-hydroxy-3(2H)-furanone in the Maillard reaction. *Food Chem.* **2009**, *115*, 233-237.
- Werkhoff, P.; Brennecke, S.; Bretschneider, W.; Bertram, H.-J. Modern methods for isolating and quantifying volatile flavor and fragrance compounds. *Food Sci. Tech.* **2002**, *115*, 139-204.

Yun, H.-M.; Jin, P.; Park, K.-R.; Hwang, J.; Jeong, H.-S.; Kim, E.-C.; Jung, J.-K.; Oh, K.-W.; Hwang, B. Y.; Han, S. B.; Hong, J. T. Thiacremonone potentiates anti-oxidant effects to improve memory dysfunction in an APP/PS1 transgenic mice model. *Mol. Neurobio.* **2016**, *53*, 2409-2420.

Zamora, R.; Aguilar, I.; Hidalgo, F. J. Epoxyalkenal-trapping ability of phenolic compounds. *Food Chem.* **2017**, *237*, 444-452.

Zhang, Y.; Ho, C. -T. Comparison of the volatile compounds formed from the thermal reaction of glucose with cysteine and glutathione. *J. Agric. Food Chem.* **1991**, *39*, 2548-2560.

Zhang, Y.; Dorjpalam, B.; Ho, C. -T. Contribution of peptides to volatile formation in the Maillard reaction of casein hydrolysate with glucose. *J. Agric. Food Chem.* **1992**, *40*, 2467-2471.

Zheng, Y.; Brown, S.; Ledig, W. O.; Mussinan, C; Ho, C. -T. Formation of sulfur-containing flavor compounds from reactions of furaneol and cysteine, glutathione, hydrogen sulfide, and alanine/hydrogen sulfide. *J. Agric. Food Chem.* **1997**, *45*, 894-897.

Zhu, Y.; Yaylayan, V. A. Interaction of free arginine and guanidine with glucose under thermal processing conditions and formation of Amadori-derived imidazolones. *Food Chem.* **2017**, *220*, 87-92

Appendix

Additional Details for Partition Coefficient Measurements

- Methanol, HPLC grade (Fisher Scientific)
- Water, HPLC grade (Fisher Scientific)
- Agilent HPLC 1100/ diode array detector (UV) at 210nm
- Graduated measuring cylinder, 1000cc.
- Zorbax Eclipse DBX-C8 column (4.6 x 150 mm, 5 μ m, Part # 993967-906)
- Benzyl alcohol, Sigma Aldrich (CAS 100-51-6; 98%)
- Cinnamic alcohol, Sigma Aldrich (CAS 104-54-1; 98%)
- N-butyl benzene, Sigma Aldrich (CAS 104-51-8; 99%)
- Allyl phenyl ether, Sigma Aldrich (CAS 1746-13-0; 99%)
- 4-4' DDT, Sigma Aldrich (CAS 50-29-3; 99%)
- Benzyl Benzoate, Sigma Aldrich (CAS 120-51-4; 99%)
- Formamide, sigma-Aldrich (CAS 75-12-7; 99.5%)
- Other appropriate reference standards (see table below)

Preparation of HPLC Mobile Phase. Mobile phase is prepared by mixing HPLC grade methanol with HPLC grade water 3:1 (v/v) ratio. In a 1000cc graduated cylinder, accurately measure 750 mL of HPLC grade methanol and pour it in mobile phase reservoir, then add 250 mL of HPLC grade water. Mix water and methanol until all the bubbles disappear.

Preparation of Reference Standards. To relate the measured capacity factor (k) of the test material with its P_{ow} , five structurally significant reference standards are selected from Table 3 and prepared according to the procedure below. An internal standard (formamide), with no retention time on the HPLC column, is used to determine the dead time (t_0) of the HPLC system.

The water solubility of a test substance is specified by the saturation mass concentration of the test substance in water at a given temperature and is expressed in g/L. Prepare a stock solution of reference standards in the mobile phase by weighing the following:

Reference Standard	Wt (g)	% in stock solution
Benzyl alcohol	0.1	1
Cinnamic alcohol	0.1	1
Allyl phenyl ether	0.1	1
Benzyl benzoate	0.1	1
N butyl benzene	0.1	1
DDT	0.1	1
Formamide	0.2	2
Mobile phase	9.7	
Total weight	10.0	

Dilute the above stock solution to prepare a working solution of reference standards by measuring 1 mL into a 100 mL volumetric flask and diluting with the mobile phase. This solution is approximately 100 ppm of each reference standard.

Preparation of Test Sample: A solution of test substance, also containing internal dead time standard (IDS) is prepared and chromatographed in duplicate, bracketed by samples of the reference mixture, using the HPLC conditions stated below. In a 4-dram vial, accurately record to the nearest decimal, the weight of the test material to 0.1 g. Tare the balance and then add 0.2 g of formamide. Dilute with 9.7 g of mobile phase. Analyze according to the HPLC conditions listed below.

Auto sampler: Agilent 1260 Autosampler
Injection Mode: Standard
Injector Volume: 10 μ l/min
Draw speed: 100 μ l/min
Eject Speed: 100 μ l/min
Pump: Agilent 1260 Quaternary pump
Column flow: 1.0ml/min
Solvents: Solvent A, Methanol (HPLC grade); Solvent B, Water (HPLC grade)
Column temp: 25 °C
Injection vol: 10 μ l
Detector: Agilent 1260 Diode Array Detector (UV) @ 210nm

Guidelines followed the Organization for Economic Co-operation and Development (OECD), OECD Guidelines for the Testing of Chemicals no. 117: "Partition Coefficient (n-octanol/water), High Performance Liquid Chromatography (HPLC) Method", April 13, 2004, as well as the European Economic Community (EEC), EEC Directive 92/69 EEC, Part A, Methods for the Determination of Physico-Chemical Properties A.8: "Partition Coefficient", EEC Publication no. L383, July 31, 1992.

Figure on $\text{Log}_{10}P_{ow}$ for standard materials.